*J. Fluid Mech.* (1983), *vol.* 133, *pp.* 83–112
*Printed in Great Britain*



# A digital technique for the simultaneous measurement of streamwise and lateral velocities in turbulent flows

By J. G. KAWALL, M. SHOKR† AND J. F. KEFFER
Department of Mechanical Engineering, University of Toronto, Canada

(Received 28 July 1982 and in revised form 24 March 1983)

A novel, digital, hot-wire anemometer technique for the simultaneous measurement of the instantaneous streamwise and lateral velocity fields in high-intensity turbulent flows is discussed. It involves the use of a three-wire probe comprising two 45° slanted hot wires and a normal hot wire. A comprehensive and systematic examination of several factors that can affect the fidelity of the streamwise and lateral velocity waveforms is developed to assess the performance of the new technique as well as hot-wire systems generally. These factors are: (i) rectification, which stems from the inherent insensitivity of hot wires to the direction of the instantaneous (total) velocity vector in a turbulent flow; (ii) spanwise velocity fluctuations; (iii) axial cooling of hot wires; (iv) unpredictable variations in one of four hot-wire calibration parameters; (v) random hot-wire calibration errors; (vi) spanwise separation of the hot wires. Relevant hot-wire anemometer-response equations relating instantaneous anemometer output voltages to instantaneous flow velocities were established on the basis of extensive voltage–velocity calibration data pertaining to hot wires orientated with respect to the calibration flow velocity at various yaw and pitch angles ranging from 0° to 90°. Simulated Gaussian (streamwise, lateral and spanwise) velocity fields appropriate to flows with turbulence intensity levels varying between 5 and 80% and Reynolds shear-stress coefficients varying between 0.1 and 0.5 were generated by means of a digital computer, and the associated anemometer-voltage signals computed in accordance with the response equations subject to different combinations of the first four of the aforementioned factors. In order to take into account the effects of the last two factors, viz calibration errors and spanwise wire separation, uncorrelated Gaussian 'noise' fluctuations were superimposed on the above voltage signals. Estimates of the known (simulated) streamwise and lateral velocity signals were then determined by simultaneous solution of (*a*) the actual instantaneous response equations, (*b*) approximate versions of them, and (*c*) linearized versions of them. The results indicate that reasonably accurate estimates of velocity signals from a turbulent flow can be obtained by means of conventional hot-wire anemometer techniques – which assume that anemometer voltage fluctuations are linear functions of corresponding velocity fluctuations – only if the turbulent intensity level of the flow does not exceed about 20%. In marked contrast, the 3-wire anemometer technique introduced here can be used to measure streamwise and lateral velocity signals simultaneously with a high degree of accuracy for turbulence-intensity levels of up to 40%. In addition, this technique is capable of yielding high-fidelity streamwise velocity waveforms for levels in excess of 70%.

---

† Present address: Atmospheric Environment Services, Canada.

## 1. Introduction

The hot-wire anemometer (HWA) has been and will likely continue to be, for the forseeable future, the principal way of obtaining quantitative information on turbulent flows, although, as with many scientific measuring devices, it does have certain limitations. The basic drawback is that the accuracy depends largely upon the turbulence-intensity level of the flow, decreasing as the level increases beyond some limiting value. With respect to flows such as grid turbulence and small deficit wakes where turbulence intensities do not exceed 10 %, the majority of HWA results can be acceptably accurate – regardless of the particular HWA technique used. On the other hand, for flows such as jets and mixing layers, in which, as the HWA measurements of Gutmark & Wygnanski (1976), Davies, Keffer & Baines (1975) and Wygnanski & Fiedler (1969, 1970) have shown, turbulent-intensity levels can range from about 15 %, where the intermittency factor is unity, to levels greater than 50 %, where the intermittency factor is 0.5, to levels close to or in excess of 100 %, where the intermittency factor is of the order 0.05, the reliability of HWA data is limited, and, as we will show, is strongly influenced by the precise manner in which the HWA is used.

Until recently, HWA techniques have been exclusively analogue in nature, involving the use of specialized electronic instruments and various relationships based upon linearized forms of the nonlinear HWA response equations. The measurement of turbulent quantities in this manner usually proves to be a lengthy task, and, once the turbulence-intensity level in the flow being investigated is much greater than 20 %, the data are subject to significant errors – especially quantities involving more than one flow variable (e.g. the Reynolds shear stress). In the case of single-wire HWA data, these errors arise primarily from the neglect of second- and higher-order terms in the series expansion of the HWA response equation, in conjunction with the fact that the expansion ceases to be valid at all instants once the turbulence intensity levels exceed about 35 %. In the case of X-wire HWA data, the errors can be largely due also to wire separation. If the perpendicular distance between the 2 wires of an X-wire probe exceeds some limiting value (e.g. 1 mm when theTaylor microscale of the flow is about 10 mm), then the assumption that the wires respond to the same velocity fields on an instantaneous basis will be vitiated.

An assessment of the errors ascribable to linearization of the HWA response equations can be arrived at from a consideration of the second- and higher-order terms in the series expansions of these equations. If the turbulence-intensity level does not exceed about 20 %, then the assessment will be reasonably accurate. In contrast, if the turbulence-intensity level is well in excess of 20 %, then the assessment will be approximate at best. The details of this approach to the error analysis of HWA measurements are given by Hinze (1959). Notice that any HWA data 'correction' scheme based on or related to this approach, such as the one proposed by Rodi (1975), has little value. For if the turbulence-intensity level does not exceed10 % (and, in the case of X-wire data, wire separation is not a major factor), then, as will be shown here, application of correction factors to the data would be unnecessary. And if the turbulence-intensity level is well in excess of 20 %, then the HWA voltage statistics (e.g. the mean voltages and, in particular, the mean-square voltages) would be 'contaminated' in a highly nonlinear fashion. In consequence, it would hardly be possible to 'correct' velocity statistics derived from these voltage statistics.

With the advent of analogue-to-digital converters and high-speed digital computers, it has become possible to devise digital (and hybrid, i.e. analogue–digital) HWA

methods for the measurement of turbulent-flow signals. These enable the statistical properties of the signals to be determined in a very efficient manner. Such techniques have been developed, for example, by Keffer, Budny & Kawall (1978) for the simultaneous measurement of the instantaneous temperature and streamwise velocity fields in heated turbulent flows; by Bradbury (1978) for measuring various statistical properties of (isothermal) high-intensity turbulent flows – such as the near wakes of bluff bodies; by Foss (1978) for the measurement of the instantaneous spanwise vorticity in (isothermal) turbulent flows; and by Lakshminarayana (1982) for the simultaneous measurement of instantaneous streamwise, lateral and spanwise velocities in (isothermal) turbulent flows. It should be mentioned here that Foss's technique involves the simultaneous measurement of instantaneous streamwise and lateral velocities by means of an X-wire probe, and that Foss has carried out an analytical error analysis of the velocity signals that are obtained with such a probe in an attempt to assess the accuracy of his technique. This analysis, however, is likely to be of limited value with respect to flows having turbulent-intensity levels much in excess of 15%, inasmuch as it entails expansion of nonlinear HWA response equations and, in principle, linearization of these equations in order to determine hot-wire sensitivities. It should be mentioned as well that, with such high-intensity flows, data obtained via the Lakshminarayana method will be adversely affected by rectification, and those obtained via the Foss method by both rectification and spanwise velocity fluctuations.

In the present work, we describe a novel digital HWA technique for the simultaneous measurement of the instantaneous streamwise and lateral velocity signals in high-intensity turbulent air flows, which we feel offers advantages over other techniques in terms of flexibility, straightforwardness and, most of all, accuracy. This entails the use of (i) a 3-wire probe comprising two 45° slanted wires and a normal wire, in conjunction with 3 constant-temperature anemometer units; (ii) an analogue-to-digital converter to digitize simultaneously the analogue HWA voltage signals; and (iii) a high-speed digital computer to solve 3 nonlinear HWA response equations for the requisite instantaneous streamwise and lateral velocities, and to compute the various statistical properties. In order to establish the efficacy of our technique, we have carried out an evaluation of the errors due to six factors that can, in practice, affect the fidelity of velocity waveforms pbtained by means of the HWA. These are: (1) rectification, which occurs whenever the instantaneous velocity normal to a hot wire becomes negative; (2) spanwise velocity fluctuations, which are ignored in conventional HWA techniques; (3) axial cooling, whose effect is considered here through the use of the axial cooling parameter that was introduced by Hinze (1959) and which has been shown by Champagne, Sleicher & Wehrmann (1967) to be essentially a function of the length-to-diameter ratio of a given hot wire; (4) unpredictable variations in one of 4 hot-wire calibration parameters or 'constants', which are ascribable to the presence of the hot-wire prongs and which are likely to occur whenever the instantaneous velocity vector makes an angle of less than about 30° with a given wire; (5) random hot-wire calibration errors; (6) spanwise wire separation.

The rationale of the present HWA error assessment procedure is the same as that used by Tutu & Chevray (1975) to evaluate X-wire HWA measurements pertaining to high-intensity turbulent flows. The details of the two approaches, however, are different. Tutu & Chevray recognized that the conventional HWA error analysis is not really valid for flows having turbulence-intensity levels much above 20%. On the assumption that the factors that affect HWA signals are rectification, spanwise

velocity fluctuations and axial cooling (via the axial cooling parameter), they derived transformation equations that relate the joint probability density function (JPDF) of the actual streamwise, lateral and spanwise velocity signals of any given turbulent flow to the JPDF of the streamwise and lateral velocity signals that would be obtained, subject to the above assumption, by means of a 45° X-wire probe located in that flow. Accordingly, with the aid of a digital computer, they were able to compute various estimated or 'measured' statistical properties for a turbulent flow having a jointly Gaussian probabilistic structure (i.e. a flow with jointly Gaussian streamwise, lateral and spanwise velocities). Since the statistical properties of such a flow are known exactly once the parameters of the JPDF are specified,it was possible for them to carry out a precise evaluation of the errors associated with the 'measured' data. On the basis of the error results found by Tutu & Chevray, it is apparent that the accuracy of conventional X-wire results is likely to decrease noticeably as turbulence-intensity levels increase much beyond about 20%. In particular, these results show that, as a result of rectification and spanwise velocity fluctuations, the magnitude of the error in the Reynolds shear stress determined with an X-wire probe can increase from about 7% when the turbulence intensity level is 20% to about 50% when the level is 50%.

Although Tutu & Chevray's HWA assessment procedure is fundamentally sound, it has two important limitations, viz (i) it does not permit an examination to be made of all the factors that can affect X-wire HWA results, and (ii) it does not yield signal-to-noise ratios, and hence it fails to provide a measure of the distortion associated with the estimated velocity waveforms. Our approach, on the other hand, obviates these restrictions, inasmuch as we can simulate the streamwise, lateral and spanwise velocity fields of any turbulent flow with specified statistical properties, and then compute the corresponding estimated signals in accordance with HWA response equations that reflect the effect of virtually any relevant factor or combination of relevant factors. This means that we can determine not only signal-to-noise ratios and the errors associated with estimated moments, joint moments, probability density functions (PDFs) and JPDFs, but also the errors associated with estimated correlation functions and spectra. In addition, with the present approach, the influence of intermittency on the various errors can be investigated– since intermittent turbulent signals can be readily generated. It should be emphasized that, for any given flow conditions, if the errors associated with the estimates of moments, joint moments, PDFs and JPDFs determined with a 45° X-wire probe are due only to rectification, spanwise velocity fluctuations and axial cooling, then the present approach and Tutu & Chevray's approach will yield identical (%) error results pertaining to such statistics.

## 2. HWA response equations

Subsections 2.1–2.5 give a detailed development of the working relationships for HWA generally. In particular, §2.1 is a novel statement in that the derived equations present a complete description of the wire response without the conventional approximations.

### 2.1. *The nonlinear 3-wire response equations*

On the basis of a comprehensive set of HWA voltage/velocity calibration data, we have established (Kawall, Keffer & Shokr 1983) that when two inclined hot wires and a normal hot wire are located within an isothermal turbulent flow as depicted in figure

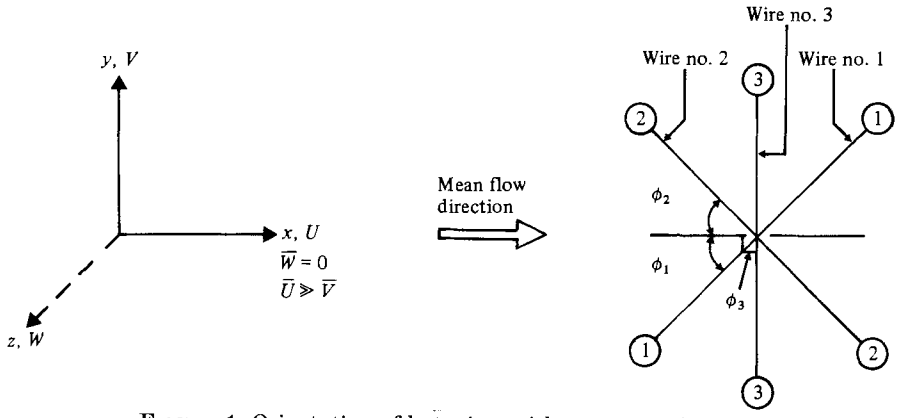


FIGURE 1. Orientation of hot wires with respect to flow.

1, and each of these wires is operated by means of a constant-temperature anemometer (CTA),† the resulting HWA response equations can be expressed as:

$$E_1^2 = A_1 + B_1\{Q_{xy_1}^2(\sin^2\theta_1 + k^2\cos^2\theta_1 + \tan^2\beta_1)\}^{\frac{1}{2}n}, \tag{2.1}$$

$$E_2^2 = A_2 + B_2\{Q_{xy_2}^2(\sin^2\theta_2 + k^2\cos^2\theta_2 + \tan^2\beta_2)\}^{\frac{1}{2}n}, \tag{2.2}$$

$$E_3^2 = A_3 + B_3\{Q_{xy_3}^2(\sin^2\theta_3 + k^2\cos^2\theta_3 + \tan^2\beta_3)\}^{\frac{1}{2}n}. \tag{2.3}$$

In these equations, which will henceforth be referred to as the nonlinear 3-wire response equations, the subscripts 1 and 2 pertain to the inclined wires (wires no. 1 and no. 2 in figure 1) and subscript 3 pertains to the normal wire (wire no. 3 in figure 1); $E_i$ is the instantaneous HWA output voltage for the $i$th wire ($i = 1, 2, 3$), which is produced by the corresponding instantaneous effective cooling velocity $\{Q_{xyi}^2(\sin^2\theta_i + k^2\cos^2\theta_i + \tan^2\beta_i)\}^{\frac{1}{2}}$;

$$Q_{xyi}^2 = U_{ti}^2 + V_{ti}^2,$$

where $U_{ti}$ and $V_{ti}$ are the 'true' components of the instantaneous flow velocity vector in the $x$- or streamwise direction and in the $y$- or lateral direction respectively; $\theta_1$, $\theta_2$ and $\theta_3$ are the instantaneous yaw angles given respectively by

$$\theta_1 = \phi_1 - \alpha_1, \quad \theta_2 = \phi_2 - \alpha_2, \quad \theta_3 = \phi_3 - \alpha_3,$$

where $\phi_1$, $\phi_2$ and $\phi_3$ are the (fixed) angles that the hot wires make with the $x$-axis (see figure 1), and $\alpha_i = \tan^{-1}(V_{ti}/U_{ti})$;

$$\tan\beta_i = W_{ti}/Q_{xyi},$$

where $\beta_i$ is the instantaneous pitch angle, and $W_{ti}$ is the 'true' component of the instantaneous flow velocity vector in the $z$- or spanwise direction; $A_i$, $B_i$, $n$ and $k$ are parameters that are determined by means of a least-squares regression analysis of the aforementioned HWA calibration data. This analysis indicates that in the case of DISA miniature platinum-plated tungsten hot wires, $A$ varies with $\theta$ as illustrated in figure 2 and, hence, is essentially constant for values of the angle between the hot wire and the instantaneous flow velocity vector that are in excess of about 25° and increases significantly as this angle decreases much below the latter value; $B$ is

† A detailed description of the CTA is given by Blackwelder (1981).

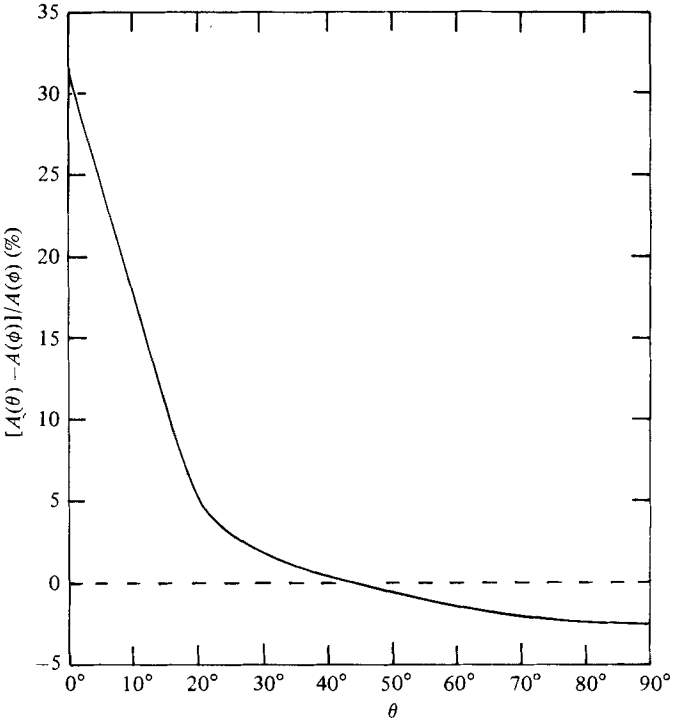


FIGURE 2. Typical variation of the hot-wire parameter $A$ with yaw angle $\theta$.

constant for all values of this angle; $n$ is a constant whose optimum value can be taken as 0.38 for mean flow velocities up to about 20 m $s^{-1}$; and $k$, which will be referred to as the axial cooling parameter, can be treated as a constant whose optimum value is about 0.1 for wires having length-to-diameter ($l/d$) ratios of 250.

On the assumption that ($a$) the lengths of the 3 hot wires and the distances separating them in the spanwise direction are sufficiently small so that $U_{t_1} = U_{t_2} = U_{t_3} = U_t$, $V_{t_1} = V_{t_2} = V_{t_3} = V_t$ and $W_{t_1} = W_{t_2} = W_{t_3} = W_t$, and ($b$) the wires are orientated so that $\phi_1 = \phi_2 = 45°$ and $\phi_3 = 90°$, (2.1), (2.2) and (2.3) become respectively

$$E_1^2 = A_1 + B_1\{\tfrac{1}{2}(U_t - V_t)^2 + \tfrac{1}{2}k^2(U_t + V_t)^2 + W_t^2\}^{\frac{1}{2}n}, \tag{2.4}$$

$$E_2^2 = A_2 + B_2\{\tfrac{1}{2}(U_t + V_t)^2 + \tfrac{1}{2}k^2(U_t - V_t)^2 + W_t^2\}^{\frac{1}{2}n}, \tag{2.5}$$

$$E_3^2 = A_3 + B_3\{U_t^2 + k^2 V_t^2 + W_t^2\}^{\frac{1}{2}n}. \tag{2.6}$$

Appropriate manipulation of these equations then yields the following expressions for $U_t^2$, $U_t V_t$ and $W_t^2$:

$$U_t^2 = \frac{Z + (Z^2 + (Z_2 - Z_1)^2)^{\frac{1}{2}}}{2(1-k^2)}, \tag{2.7}$$

$$U_t V_t = \frac{Z_2 - Z_1}{2(1-k^2)}, \tag{2.8}$$

$$W_t^2 = Z_3 - k V_t^2 - U_t^2, \tag{2.9}$$

where

$$Z_1 = \left(\frac{E_1^2 - A_1}{B_1}\right)^{2/n}, \tag{2.10}$$

$$Z_2 = \left(\frac{E_2^2 - A_2}{B_2}\right)^{2/n}, \tag{2.11}$$

$$Z_3 = \left(\frac{E_3^2 - A_3}{B_3}\right)^{2/n}, \tag{2.12}$$

$$Z = 2Z_3 - (Z_1 + Z_2). \tag{2.13}$$

In order to guarantee that any given HWA technique will yield a positive value for the mean streamwise velocity $\overline{U}_t$, one must, in effect, regard $U_t$ as always being positive – even though it can sometimes be negative, especially in high-intensity turbulent flows. Accordingly, the optimum estimates of $U_t$, $V_t$ and $W_t^2$ that are obtainable by means of the present 3-wire response equations are given respectively by

$$U_3 = |U_t| = \left[\frac{Z + (Z^2 + (Z_2 - Z_1)^2)^{\frac{1}{2}}}{2(1-k^2)}\right]^{\frac{1}{2}}, \tag{2.14}$$

$$V_3 = \frac{Z_2 - Z_1}{2(1-k^2)\,U_3}, \tag{2.15}$$

$$W_3^2 = Z_3 - k^2 V_3^2 - U_3^2. \tag{2.16}$$

The following points should be noted, *vis-à-vis* these estimates.

(1) It follows from (2.14)–(2.16) and (2.8) that, whenever $U_t > 0$,

$$U_3 = U_t, \quad V_3 = V_t;$$

but, whenever $U_t < 0$,

$$U_3 = -U_t, \quad V_3 = -V_t.$$

For this reason, we say that rectification occurs in the case of the 3-wire response equations whenever $U_t < 0$.

(2) With respect to a flow in which the turbulence-intensity level – which is defined as $u_t'/\overline{U}_t$, where $u_t'$ is the root-mean-square (r.m.s.) value of $U_t$ – exceedsabout 40 %, it can be expected that results based on these equations will be subject to significant rectification errors.

(3) In the case of an HWA technique that involves a single hot wire lying in the $(x, y)$-plane of a flow, rectification is said to occur whenever the instantaneous flow velocity component normal to the hot wire (and to the $z$-axis) becomes negative – since such a hot wire will respond principally to the magnitude of this velocity component. Thus, if the orientation of the hot wire in question is the same as that of wire no. 1 in figure 1 (with $\phi_1 = 45°$), rectification would occur whenever $U_t - V_t < 0$ (or, equivalently, $\alpha > 45°$); if the orientation is the same as that of wire no. 2 (with $\phi_2 = 45°$), rectification would occur whenever $U_t + V_t < 0$ (or equivalently $\alpha < -45°$); and if the orientation is the same as that of wire no. 3, rectification would occur whenever $U_t < 0$. In view of this, it is evident that turbulence results obtained via any HWA technique will be adversely affected by rectification once the turbulence-intensity level of the flow under investigation exceeds a limiting value which depends upon the particular HWA technique used. It turns out that this latter value is considerably greater for the present 3-wire technique than it is for any other (existing) multiwire technique (being about 35 % compared with about 20 %, with respect to flows having Gaussian velocity fields).

(4) In the evaluation of $Z_1$, $Z_2$ and $Z_3$ ((2.10),(2.11) and (2.12) respectively), $A_1$, $A_2$ and $A_3$ must be treated as constants. Consequently, for flows with values of $u_t'/\overline{U}_t$ in excess of 15 %, the accuracy of turbulence results based on (2.14)–(2.16) will be

impaired by the actual, unpredictable variations in $A_1$, $A_2$ and $A_3$ (i.e. random '$A$' variations) that arise when $u_t'/\overline{U}_t$ is greater than about 15%.

(5) Deviations in $\phi_1$ and $\phi_2$ from 45° and in $\phi_3$ from 90° up to about $\pm 1°$ will have virtually no adverse effect on the accuracy of the aforementioned estimates ($U_3$, $V_3$ and $W_3^2$).

(6) Once $\phi_1 = \phi_2$ and $\phi_3 = 90°$, explicit expressions for $U_t^2$, $U_t V_t$ and $W_t^2$, similar to those given by (2.7)–(2.9), can be readily derived from (2.1)–(2.3).

### 2.2. *The nonlinear* X*-wire response equations*

With respect to two 45° inclined hot wires (or a 45° X-wire probe) orientated within an isothermal flow as depicted in figure 1 and used in conjunction with two CTAs, the HWA response equations can be taken as (2.4) and (2.5). It follows from these equations, which will henceforth be referred to as the nonlinear X-wire response equations, that

$$U_t = R_1 + R_2, \tag{2.17}$$

$$V_t = R_2 - R_1, \tag{2.18}$$

where

$$R_1 = \pm\left[\frac{(Z_1 - W_t^2) - k^2(Z_2 - W_t^2)}{2(1-k^4)}\right]^{\frac{1}{2}}, \tag{2.19}$$

$$R_2 = \pm\left[\frac{(Z_2 - W_t^2) - k^2(Z_1 - W_t^2)}{2(1-k^4)}\right]^{\frac{1}{2}}. \tag{2.20}$$

The above expressions serve to show clearly that, in general, if one wants to determine estimates of $U_t$ and $V_t$ using X-wire anemometry (i.e. via (2.1) and (2.2)), then $W_t$ must be taken to be zero – so as to permit evaluation of either $R_1^2$ and $R_2^2$, or their equivalents when $\phi_1$ and $\phi_2$ differ from 45° – and the signs of $R_1$ and $R_2$, or their equivalents, must be prescribed. Now, for the same reason given in connection with (2.14)–(2.16), it is assumed that the positive signs in (2.19) and (2.20) always apply. Thus the optimum estimates of $U_t$ and $V_t$ that can be obtained by means of the present nonlinear X-wire response equations are given respectively by

$$U_X^* = |R_1^*| + |R_2^*|, \tag{2.21}$$

$$V_X^* = |R_2^*| - |R_1^*|, \tag{2.22}$$

where

$$R_1^* = \pm\left[\frac{(Z_1 - k^2 Z_2)}{2(1-k^4)}\right]^{\frac{1}{2}}, \tag{2.23}$$

$$R_2^* = \pm\left[\frac{(Z_2 - k^2 Z_1)}{2(1-k^4)}\right]^{\frac{1}{2}}. \tag{2.24}$$

The following points should be noted here.

(1) It follows from (2.21)–(2.24) and (2.8) that

$$U_X^* V_X^* = U_t V_t.$$

Furthermore, if (*a*) the values of both $R_1^*$ and $R_2^*$ always remain positive, (*b*) $w$-fluctuations are negligibly small, and (*c*) $A$-variations (and any other sources of error) are absent, then

$$U_X^* = U_t, \quad V_X^* = V_t.$$

On the other hand, if the value of either $R_1^*$ or $R_2^*$ becomes negative, or the $w$-fluctuations are significantly large, or $A$-variations occur, then

$$U_{\mathsf{X}}^* \neq U_t, \quad V_{\mathsf{X}}^* \neq V_t,$$

i.e. the X-wire response equations will yield incorrect values of $U_t$ and $V_t$.

(2) On the assumption that both $k$ and $W_t$ are negligibly small, (2.21) and (2.22) become respectively

$$U_{\mathsf{X}}^{**} = |R_1^{**}| + |R_2^{**}|, \tag{2.25}$$

$$V_{\mathsf{X}}^{**} = |R_2^{**}| - |R_1^{**}|, \tag{2.26}$$

where

$$R_1^{**} = \pm(\tfrac{1}{2}Z_1)^{\frac{1}{2}}, \tag{2.27}$$

$$R_2^{**} = \pm(\tfrac{1}{2}Z_2)^{\frac{1}{2}}. \tag{2.28}$$

Hence, by virtue of (2.8),

$$U_{\mathsf{X}}^{**}\, V_{\mathsf{X}}^{**} = U_t\, V_t(1-k^2). \tag{2.29}$$

(3) The estimates of $U_t$ and $V_t$ used by Tutu & Chevray (1975), viz $u^*$ and $v^*$, are related to $U_{\mathsf{X}}^{**}$ and $V_{\mathsf{X}}^{**}$ as follows:

$$u^* = \frac{U_{\mathsf{X}}^{**}}{(1+k^2)^{\frac{1}{2}}}, \quad v^* = \frac{V_{\mathsf{X}}^{**}}{(1+k^2)^{\frac{1}{2}}}.$$

Hence, by virtue of (2.29),

$$u^*v^* = \frac{U_t\, V_t(1-k^2)}{1+k^2}.$$

(4) Given that both $W_t$ and $k$ are zero, $U_{\mathsf{X}}^{**}$ and $V_{\mathsf{X}}^{**}$ will be related to $U_t$ and $V_t$ as follows:

$$U_{\mathsf{X}}^{**} = \tfrac{1}{2}[|U_t + V_t| + |U_t - V_t|],$$

$$V_{\mathsf{X}}^{**} = \tfrac{1}{2}[|U_t + V_t| - |U_t - V_t|].$$

Hence, whenever $U_t > |V_t|$,

$$U_{\mathsf{X}}^{**} = U_t, \quad V_{\mathsf{X}}^{**} = V_t;$$

but, whenever $U_t < |V_t|$,

$$U_{\mathsf{X}}^{**} = -U_t \text{ or } +V_t \text{ or } -V_t,$$

and

$$V_{\mathsf{X}}^{**} = -V_t \text{ or } +U_t \text{ or } -U_t.$$

In view of this, we say that rectification occurs in the case of the 45° X-wire response equations whenever $U_t < |V_t|$, or equivalently $|\alpha| > 45°$.

(5) The frequency of occurrence of the condition $U_t < 0$, which defines rectification in the case of the 3-wire response equations, will always be considerably smaller than the frequency of occurrence of the condition $U_t < |V_t|$. Also, the $U$- and $V$-estimates obtained via the 3-wire response equations will not be affected by $w$ fluctuations, whereas those obtained via any X-wire equations will be. Consequently, for any flow having values of $u_t'/\overline{U}_t$ in excess of about 15%, the '3-wire' estimates will be more accurate than the 'X-wire' estimates.

### 2.3. *The nonlinear normal-wire response equation*

With respect to a normal hot wire orientated within a turbulent flow as depicted in figure 1, and used in conjunction with a CTA, the HWA response equation can be

taken as (2.6). It follows from this equation, which will henceforth be referred to as the nonlinear normal-wire response equation, that

$$U_t = \pm(Z_3 - k^2 V_t^2 - W_t^2)^{\frac{1}{2}}. \tag{2.30}$$

Clearly the optimum estimate of $U_t$ that is obtainable by means of (2.30) is given by

$$U_N = Z_3^{\frac{1}{2}}. \tag{2.31}$$

Notice that, if both $W_t$ and $k$ are negligibly small, then

$$U_N = U_t.$$

Hence, whenever $U_t > 0$,

$$U_N = U_t;$$

but, whenever $U_t < 0$,

$$U_N = -U_t.$$

Therefore rectification occurs in the case of the normal-wire response equation whenever $U_t < 0$. Notice as well that since the frequency of occurrence of the latter condition will always be considerably smaller than the frequency of occurrence of the condition $U_t < |V_t|$, it is likely that $U_n$ will be a more reliable estimate of $U_t$ than will either $U_X^{**}$ (see (2.25)) or $U_X^*$ (see (2.21)).

### 2.4. *The mean and linearized* X*-wire response equations*

The general form of the constant-temperature HWA response equation is given by

$$E^2 = A + BQ_C^n, \tag{2.32}$$

where

$$E = \overline{E} + e, \quad Q_C = \overline{Q}_C + q_C;$$

and $A$, $B$ and $n$ are calibration parameters. If $|q_C|$ is always less than $\overline{Q}_c$ then $Q_C^n$ can be expanded about $\overline{Q}_C$, yielding

$$\overline{E}^2 + 2e\overline{E} + e^2 = A + B\overline{Q}_C^n\left[1 + \frac{nq_C}{\overline{Q}_C} + \ldots\right]. \tag{2.33}$$

In the case of an X-wire probe located within a turbulent flow in such a way that its inclined hot wires, wires no. 1 and no. 2, are orientated as in figure 1, it follows from (2.33) that, if the local turbulence-intensity levels of the flow do not exceed about 10%, then the mean and fluctuating components of the HWA output voltages for wires no. 1 and no. 2 are given by

$$\overline{E}_1^2 = A_1 + B_1\overline{Q}_{C_1}^n, \tag{2.34}$$

$$e_1 = \frac{nB_1}{2\overline{E}_1\overline{Q}_{C_1}^{1-n}} q_{C_1} = S_1 q_{C_1}, \tag{2.35}$$

$$\overline{E}_2^2 = A_2 + B_2\overline{Q}_{C_2}^n, \tag{2.36}$$

$$e_2 = \frac{nB_2}{2\overline{E}_2\overline{Q}_{C_2}^{1-n}} q_{C_2} = S_2 q_{C_2}. \tag{2.37}$$

These equations are the so-called mean and linearized X-wire response equations, and they yield the following estimates of $U_t$ and $V_t$ when $\phi_1 = \phi_2 = \phi$:

$$U_{XL} = \overline{U}_{XL} + u_{XL} = \frac{\overline{Q}_{C_1} + \overline{Q}_{C_2} + q_{C_1} + q_{C_2}}{2a} \tag{2.38}$$

$$V_{\mathrm{xL}} = \overline{V}_{\mathrm{xL}} + v_{\mathrm{xL}} = \frac{\overline{Q}_{\mathrm{C}_2} - \overline{Q}_{\mathrm{C}_1} + q_{\mathrm{C}_2} - q_{\mathrm{C}_1}}{2b}, \tag{2.39}$$

where

$$a = (\sin^2\phi + l^2\cos^2\phi)^{\frac{1}{2}}, \quad b = \frac{\sin^2\phi(1-k^2)}{2a}.$$

It should be noted here that for any flow whose local turbulence intensity levels do not exceed about 10 % (i.e. any *low-intensity* turbulent flow), $U_{\mathrm{xL}}$ and $V_{\mathrm{xL}}$ will closely approximate $U_{\mathrm{t}}$ and $V_{\mathrm{t}}$ respectively; but for high-intensity turbulent flows, $U_{\mathrm{xL}}$ and $V_{\mathrm{xL}}$ will be unreliable estimates.

### 2.5. *The mean and linearized normal-wire response equations*

In the case of a normal hot wire orientated within a *low-intensity* turbulent flow as depicted in figure 1, it follows from (2.33) that the mean and fluctuating components of the associated HWA output voltage are given respectively by

$$\overline{E}^2 = A + B\overline{Q}_{\mathrm{C}}^n, \tag{2.40}$$

$$e = \frac{nB}{2\overline{E}\overline{Q}_{\mathrm{C}}^{1-n}} q_{\mathrm{C}} = Sq_{\mathrm{C}}. \tag{2.41}$$

These equations, which are the so-called mean and linearized normal-wire response equations, yield the following estimate of $U_{\mathrm{t}}$:

$$U_{\mathrm{NL}} = \overline{U}_{\mathrm{NL}} + u_{\mathrm{NL}} = \overline{Q}_{\mathrm{C}} + q_{\mathrm{C}}.$$

## 3. Basic aspects of the 3-wire HWA technique

The essence of the present 3-wire HWA technique for the simultaneous measurement of $U$- and $V$-signals in high-intensity turbulent flow is the determination of digital versions of the analogue signals $U_3$ and $V_3$ defined by (2.14) and (2.15). Thus this technique relies on the use of a 3-wire probe comprising a normal hot wire and two 45° inclined hot wires (see figure 3), in conjunction with 3 constant-temperature anemometers, and involves the following steps.

(1) Calibration of the 3-wire probe for the purpose of evaluating the various parameters that appear in (2.4)–(2.6) (viz the $A$s, $B$s, $n$ and $k$).

(2) Simultaneous conversion of analogue voltage signals corresponding to the HWA voltages $E_1$, $E_2$ and $E_3$ given by (2.4)–(2.6) into digital voltage signals. (This is accomplished by means of an analogue-to-digital converter.)

(3) Transformation of these digital signals into data sequences, $Z_{1j}$, $Z_{2j}$ and $Z_{3j}$ ($j = 1, 2, \ldots$), representing the quantities $Z_1$, $Z_2$ and $Z_3$ defined by (2.10)–(2.12). (This is done with the aid of a digital computer.)

(4) Manipulation of $Z_{1j}$, $Z_{2j}$ and $Z_{3j}$ in accordance with (2.13)–(2.15), for the purpose of generating the requisite digital signals $U_{3j}$ and $V_{3j}$. (This too is done with the aid of a digital computer.)

## 4. Simulation details

### 4.1. *Signal generation and flow characteristics*

The HWA response, as described by the full equations (§2), is complex and highly nonlinear. It was thus decided that a precise and controlled assessment of HWA techniques could only be effected by simulation of specific turbulent flows, especially for cases of high intensity.

Following Tutu & Chevray (1975), we considered simulated flows with

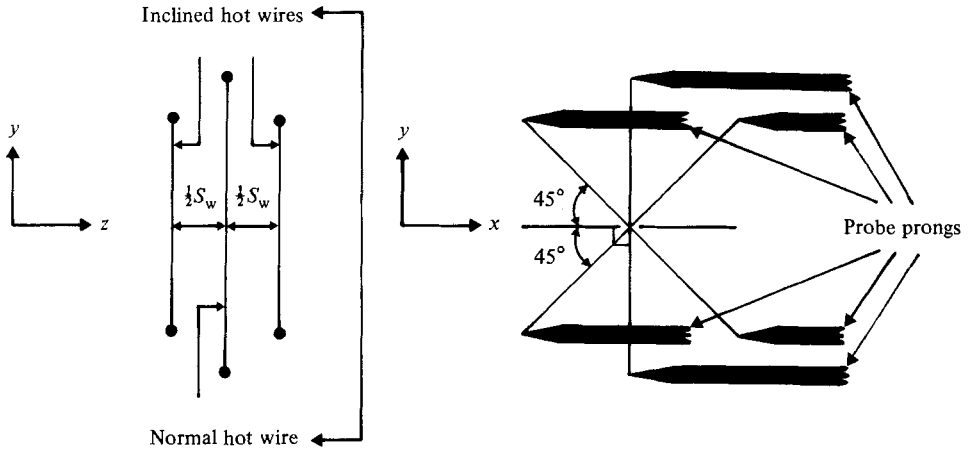


FIGURE 3. Schematic diagram of the 3-wire probe.

$\overline{W} = \overline{uw} = \overline{vw} = 0$, $\overline{uv} \neq 0$ and Gaussian $u$-, $v$- and $w$-signals, so that the JPDF pertaining to these flows is given by

$$p(u,v,w) = p_0 \exp\left\{-\left[\left(\frac{u}{u'}\right)^2+\left(\frac{v}{v'}\right)^2+\left(\frac{w}{w'}\right)^2-2\rho_{uv}\frac{uv}{u'v'}\right]\Big/2(1-\rho_{uv}^2)\right\},$$

where

$$p_0 = [(u'v'w')^2(2\pi)^3(1-\rho_{uv}^2)]^{-\frac{1}{2}},$$

$$\rho_{uv} = \frac{\overline{uv}}{u'v'}, \quad u = U-\overline{U}, \quad v = V-\overline{V}.$$

An IBM 3033 digital computer was used, in conjunction with FORTRAN software, to generate $N$-point digital versions of the Gaussian velocity signals. Estimates were computed in accordance with the expressions given in §2 and error data appropriate to flow situations characterized by values of $u'/\overline{U}$ ranging from 5 to 80% were determined. The following selected values of the other relevant flow parameters were used: 2 m s$^{-1}$ and 10 m s$^{-1}$ for $\overline{U}$; 0, 0.01 and 0.02 for $\overline{V}/\overline{U}$; 0.8 and 1.0 for $v'/u'$ and $w'/u'$; and 0.1, 0.3 and 0.5 for $\rho_{uv}$. $N$ was 100000, which was large enough so that the PDF of each of the $N$-point digital signals considered here conformed to the standardized Gaussian PDF,

$$p(z) = (2\pi)^{-\frac{1}{2}}\exp(-\tfrac{1}{2}z^2).$$

Thus the statistical variability of the error results (which depends upon $N$) can be ignored.

### 4.2. *Factors affecting HWA data*

The effects of six factors were investigated viz (i) rectification, (ii) $w$-fluctuations, (iii) axial cooling, (iv) $A$-variations, (v) calibration errors, and (vi) wire separation, and the following procedure was used to determine their effects upon various turbulence results.

(1) Digital velocity signals pertaining to prescribed Gaussian flow fields were generated (see §4.1).

(2) Digital voltage signals corresponding to the velocity signals generated in step 1 were determined via (2.4)–(2.6) subject to selected conditions, e.g. the absence of $w$-fluctuations and/or the absence of axial cooling. (The particular conditions used were contingent upon the effect or effects to be determined.)

(3) In the case of the effect of calibration errors, a (randomly) distorted version of each of the voltage signals obtained by means of the nonlinear HWA response equations (2.4)–(2.6) was computed in accordance with the following expression:

$$E^* = E + \Delta e_c' z_c,$$

where $E$ represents the signal obtained via (2.4), (2.5) or (2.6); $E^*$ is the distorted version of $E$; $\Delta e_c' z_c$ represents a zero-mean, random perturbation voltage signal; $\Delta e_c'$ is the calibration r.m.s. voltage error for a given wire; and $z_c$ is a standardized zero-mean Gaussian signal, for which the r.m.s. value $z_c'$ is unity.

(4) In the case of the effect of wire separation, a distorted version of each of the voltage signals obtained by means of (2.4) and (2.5), which pertain to the inclined hot wires (wires no. 1 and no. 2) in figure 1, was computed in accordance with the following expression:

$$E^* = E + \Delta e_s' z_s,$$

where $E$ represents the signal obtained via (2.4) or (2.5); $E^*$ is the distorted version of $E$; $\Delta e_s' z_s$ is a zero-mean random perturbation voltage signal that represents the difference between the instantaneous voltages produced by two identical inclined hot wires located within a turbulent flow at points separated in the spanwise direction by a distance of $\frac{1}{2}S_w$ (see figure 3); $\Delta e_s'$ is the r.m.s. value of the perturbation signal; and $z_s$ is a standardized zero-mean Gaussian signal.

(5) In the case of the combined effect of calibration errors and wire separation, a distorted version of each of the voltage signals obtained by means of (2.4) and (2.5) was computed in accordance with the following expression:

$$E^* = E + \Delta e_c' z_c + \Delta e_s' \Delta z_s.$$

(6) The voltage signals obtained in steps 2–5 were manipulated in accordance with the expressions given in §2, and thus various estimates of the velocity signals generated in step 1 were derived.

(7) Various error quantities (see §5) were evaluated.

In step 2 we employed values of $k$ equal to 0.1 and 0.15; in steps 3 and 5 values of $\Delta e_c'$ equal to $0.001E_0$ and $0.004E_0$, where $E_0$ is the square root of $A(\phi)$, the reference value of $A$ for a given hot wire (see figure 2); and, in steps 4 and 5, values of $\Delta e_s'$ equal to $0.07e'$ and $0.14e'$, where $e'$ is the r.m.s. voltage pertaining to a given hot wire and a given flow situation.

It should be pointed out that the aforementioned values of $k$ and $\Delta e_c'$ were chosen on the basis of our HWA calibration data (Kawall *et al.* 1983). These latter indicate that with respect to typical 5 μm diameter hot wires: (*a*) if the $l/d$ ratio of a wire is about 250 then the optimum value of $k$ is about 0.1 rather than the value based on the findings of Champagne *et al.* (1967), which lies between about 0.15 and 0.20; (*b*) the minimum value of $\Delta e_c'$ is about $0.001E_0$, which corresponds to $n \approx 0.38$; and (*c*) the value of $\Delta e_c'$ corresponding to the $n$-value of 0.45 advocated by Collis & Williams (1959) and others is about $0.004E_0$. Also, once the ratio of the spanwise distance separating two adjacent hot wires located at points $(x, y, z_A)$ and $(x, y, z_B)$ within a turbulent flow to the Taylor microscale pertaining to these points does not exceed approximately 0.2, the following relationship will exist between this ratio and $\Delta e_s'/e'$ (see Kawall *et al.* 1983):

$$\frac{\Delta e_s'}{e'} \approx 0.7 \frac{S_w}{\lambda_g},$$

where $\frac{1}{2}S_W = z_A - z_B$, and $\lambda_g$ is the Taylor microscale in question. Thus the above values of $\Delta e_s'$ (viz $0.07e'$ and $0.14e'$) correspond to values of $S_W/\lambda_g$ equal to 0.1 and 0.2.

## 5. Error-evaluation details

Estimates of the following basic statistical properties of turbulent shear flows were examined: mean streamwise and lateral velocities ($\overline{U}$ and $\overline{V}$), r.m.s. streamwise, lateral and spanwise velocities ($u'$, $v'$ and $w'$), Reynolds shear stress $\overline{uv}$ and turbulence-intensity levels $u'/\overline{U}$. The error associated with any of these estimates is given by

$$\epsilon_P = \frac{P_e - P_t}{P_t},$$

where $P_t$ denotes a true (or exact) statistical property and $P_e$ the corresponding estimated property.

In order to gauge the fidelity of the estimates velocity signals obtained by means of the various HWA response equations established in §2, we required a rational and objective measure of the distortion associated with the fluctuating components of these signals. The measure used here is referred to as the signal-distortion parameter (SDP), and, with reference to a true velocity signal $Q_t$ and a corresponding estimated velocity signal $Q_e$, it is given by

$$\overline{\epsilon_q^2} = \frac{\overline{(q_e - q_t)^2}}{\overline{q_t^2}}.$$

Here $q_t$ and $q_e$ are the fluctuating components of $Q_t$ and $Q_e$ respectively, i.e. $q_t = Q_t - \overline{Q}_t$ and $q_e = Q_e - \overline{Q}_e$, where $\overline{Q}_t$ and $\overline{Q}_e$ are the mean values of $Q_t$ and $Q_e$ respectively; $\overline{(q_e - q_t)^2}$ is the mean-square error associated with $q_e$, and $\overline{q_t^2}$ is the mean-square value of $q_t$. The following points, *vis-à-vis* the SDP, are of significance.

(1) If $q_e$ is identical with $q_t$ then the SDP will be zero.

(2) As the distortion associated with $q_e$ increases, the SDP will increase as well.

(3) Expansion of the above expression for the SDP yields

$$\overline{\epsilon_q^2} = 1 + (1 + \epsilon_{q'})^2 - 2r(1 + \epsilon_{q'}),$$

where $\epsilon_{q'}$ is the error in the estimated r.m.s. value of $q_e$, i.e. $\epsilon_{q'} = (q_e' - q_t')/q_e'$, and $r$ is the (linear) correlation coefficient of $q_e$ and $q_t$, i.e. $r = \overline{q_e q_t}/q_e' q_t'$. Now, we can consider $q_e$ and $q_t$ to be related as follows: $q_e = cq_t + n$, where $c$ is a positive-valued constant and $n$ is a zero-mean noise signal that is statistically independent of $q_t$. Accordingly, if $q_e$ and $q_t$ are poorly correlated but have much the same r.m.s. values (which is possible), then $r \ll 1$, $\epsilon_{q'} \approx 0$, SDP $\approx 2$, and $q_e$ will be a distorted version of $q_t$; moreover, if $q_e$ and $q_t$ are highly correlated but have significantly different r.m.s. values (which would mean that $q_t$ is either attenuated or amplified and $n \approx 0$), then $r \approx 1, \epsilon_{q'} \approx (c-1)$, SDP $\approx (c-1)^2$ and, again, $q_e$ will be a distorted version of $q_t$. Thus we see that, unlike the SDP, the error associated with an estimated r.m.s. velocity is not at all the appropriate measure of signal distortion, nor is the correlation coefficient pertaining to measured and exact velocity signals an entirely valid measure.

In the light of these details, it is clearly evident that the assessment of any particular HWA technique should be based not only on errors associated with estimated statistical properties, but also on SDPs, and that the errors associated with estimated r.m.s. velocities are not really pertinent to such an assessment. (It may be remarked that these latter errors can be of importance in the case of a comparison of 2 HWA methods that yield approximately the same SDPs.)

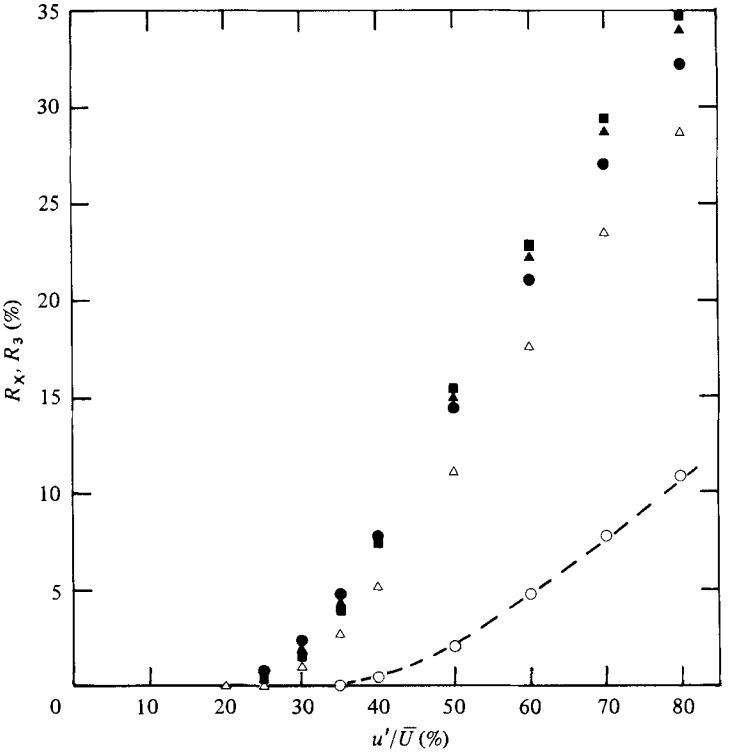


FIGURE 4. Effects of flow parameters on X-wire and 3-wire rectification. $R_X$: ■, $\overline{V}/\overline{U} = 0.005$, $v'/u' = 1.0$, $\rho_{uv} = 0.1$; ▲, 0.01, 1.0, 0.3; ●, 0.02, 1.0, 0.5; △, 0, 0.8, 0.3. $R_3$: ○; ---, based on the standardized Gaussian PDF.

## 6. Results and discussion

### 6.1. *Effects of flow parameters on HWA rectification*

Figure 4 illustrates the effects of relevant flow parameters (viz $u'/\overline{U}$, $\overline{V}/\overline{U}$, $v'/u'$ and $\rho_{uv}$) upon the occurrence of rectification with respect to our 3-wire probe and with respect to a 45° X-wire probe when these probes are located within Gaussian flows. $R_3$ denotes the frequency of occurrence of the condition $U_t < 0$ which defines rectification for the 3-wire probe, and $R_X$ the frequency of occurrence of the condition $U_t < |V_t|$, which defines rectification for the X-wire probe. As expected, $R_3$ and $R_X$ increase as $u'/\overline{U}$ increases beyond certain limiting values, below which they are zero. In the case of $R_3$, the limiting value of $u'/\overline{U}$ is about 35%; on the other hand, in the case of $R_X$ it is about 20%. We note that the variation of $R_3$ with $u'/\overline{U}$ based on the actual (digital) $U$-signals used in the present work conforms to its variation predicted by means of the standard Gaussian PDF (in accordance with the fact that these signals were Gaussian in nature).

### 6.2. *Effects of error-producing factors on* X*-wire error data*

The effects of rectification, $w$-fluctuations, axial cooling, $A$-variations, calibration errors and wire separation upon the SDPs associated with the estimated $U$- and $V$-signals obtained by means of the nonlinear 45° X-wire equations (2.4) and (2.5), and the errors associated with the basic statistical properties of these signals (see §5) are depicted in figures 5–11. The relevant parameters and their values are $\overline{U} = 10$ m s$^{-1}$; $\overline{V}/\overline{U} = 0.1$; $v'/u' = w'/u' = 1.0$, $\rho_{uv} = 0.3$, the axial cooling parameter

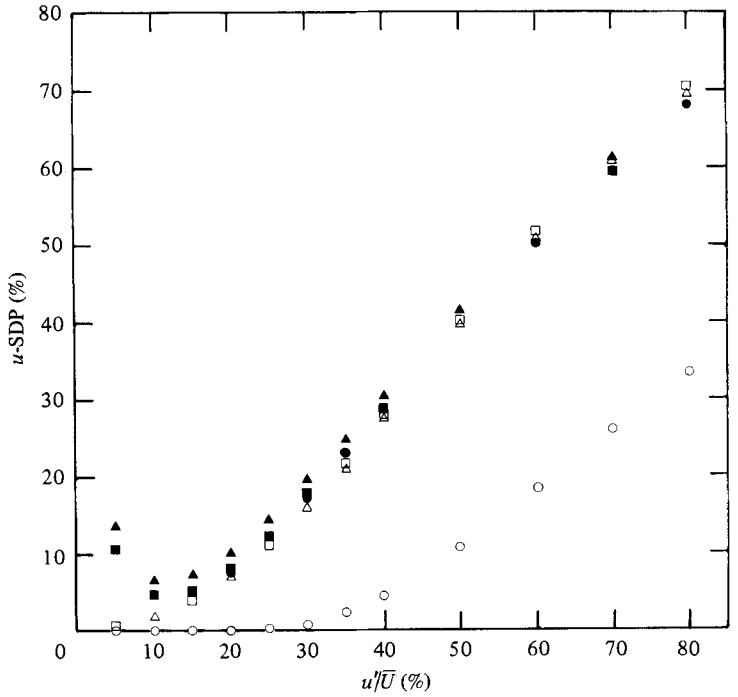


FIGURE 5. Effects of error-producing factors on the $u$-SDP pertaining to the nonlinear X-wire response equations. Relevant parameters: $\overline{U} = 10\ \mathrm{m\ s^{-1}}$, $\overline{V}/\overline{U} = 0.01$, $v'/u' = w'/u' = 1.0$, $\rho_{uv} = 0.3$, $k = 0.1$, $\Delta e_c'/E_0 \approx 0.004$, $S_w/\lambda_g \approx 0.2$. ○, rectification; □, preceding factor plus $w$-fluctuations; △, preceding factors plus axial cooling; ●, preceding factors plus $A$-variations; ■, preceding factors plus calibration errors; ▲, preceding factors plus wire separation.

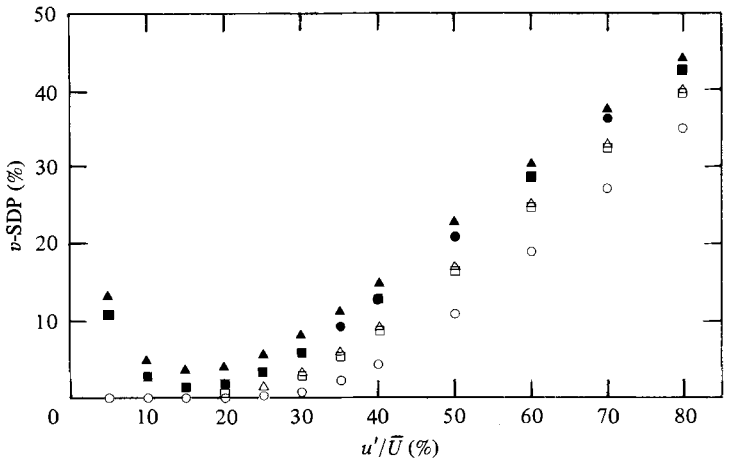


FIGURE 6. Effects of error-producing factors on the $v$-SDP pertaining to the nonlinear X-wire response equations. (The relevant parameters are the same as in figure 5, and the symbols have the same meaning.)

$k = 0.1$, the calibration-error parameter $\Delta e_c'/E_0 \approx 0.004$, which is likely to be the minimum value appropriate to a flow situation in which an $n$-value of about 0.45 is used when, in fact, the optimum $n$-value is 0.38, the wire-separation parameter $\Delta e_s'/e' \approx 0.14$, which would apply to a flow situation in which the Taylor microscale $\lambda_g$ does not exceed about 5 mm, and the wire separation $S_w$ is about 1 mm. These figures illustrate the following.

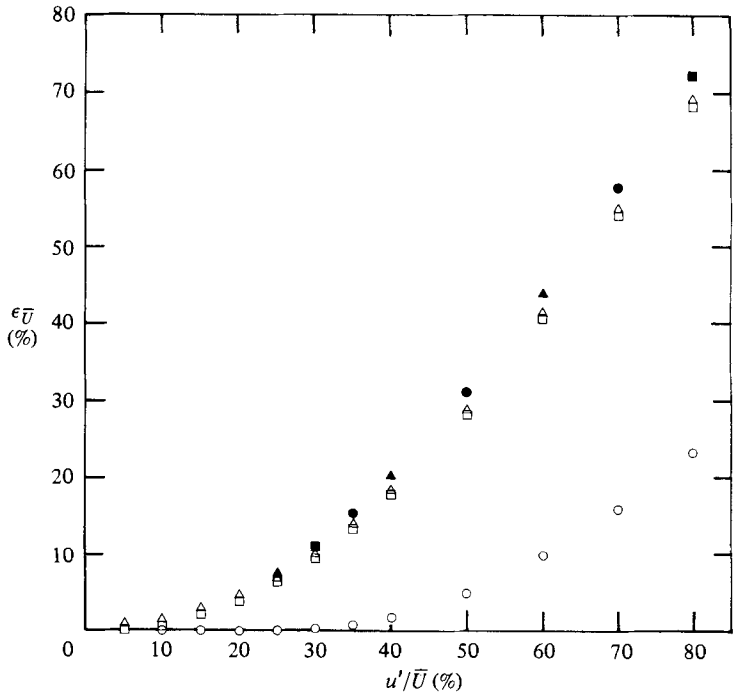


FIGURE 7. Effects of error-producing factors on $\epsilon_{\overline{U}}$ pertaining to the nonlinear X-wire response equations. (The relevant parameters are the same as in figure 5, and the symbols have the same meaning.)

(1) When all the above six factors that can adversely affect X-wire data are present: (*a*) the minimum value of the $u$-SDP will be about 7 % (figure 5), and that of the $v$-SDP about 4 % (figure 6); (*b*) $\overline{U}$ will be overestimated for any (relevant) value of $u'/\overline{U}$ (figure 7); (*c*) $\overline{V}$ will be underestimated for $u'/\overline{U}$ less than about 20 %, and overestimated for $u'/\overline{U}$ in excess of this value (figure 8); (*d*) $u'$ will be overestimated for $u'/\overline{U}$ less than about 20 %, and underestimated for $u'/\overline{U}$ in excess of this value (figure 9); (*e*) $v'$ will be overestimated for $u'/\overline{U}$ less than about 10 %, and underestimated for $u'/\overline{U}$ in excess of this value (figure 10); and (*f*) $\overline{uv}$ will be overestimated for $u'/\overline{U}$ less than about 15 % and underestimated for $u'/\overline{U}$ in excess of this value (figure 11).

(2) If $u'/\overline{U}$ does not exceed about 20 %, then the error associated with any of the basic statistical properties under consideration will be less than 10 %.

(3) As $u'/\overline{U}$ increases beyond roughly 20 %, it and $v'/u'$ will be increasingly underestimated.

(4) As $u'/\overline{U}$ increases, all X-wire data will become progressively inaccurate to the extent that they will be quite unreliable once $u'/\overline{U}$ is much in excess of 30 %. For instance, when $u'/U = 40$ %, it is entirely possible that (with all the above error-producing factors present): (*a*) the $u$-SDP (figure 5) will be about 31 % – which means that the estimated $u$-waveform is likely to bear little resemblance to the actual $u$-waveform; (*b*) $\epsilon_{\overline{U}}$ (figure 7) will be about 20 %; (*c*) $\epsilon_{\overline{V}}$ (figure 8) will be well in excess of 100 %; (*d*) $|\epsilon_{v'}|$ (figure 11) will be about 24 %; and (*e*) $|\epsilon_{\overline{uv}}|$ (figure 11) will be about 41 %.

(5) When $u'/\overline{U}$ is less than about 15 %, the dominant error-producing factors are calibration errors and wire separation. These factors, in combination, can cause the $u$- and $v$-SDPs to range from about 6 % for $u'/\overline{U} = 10$ % to about 15 % for $u'/\overline{U} = 5$ %,

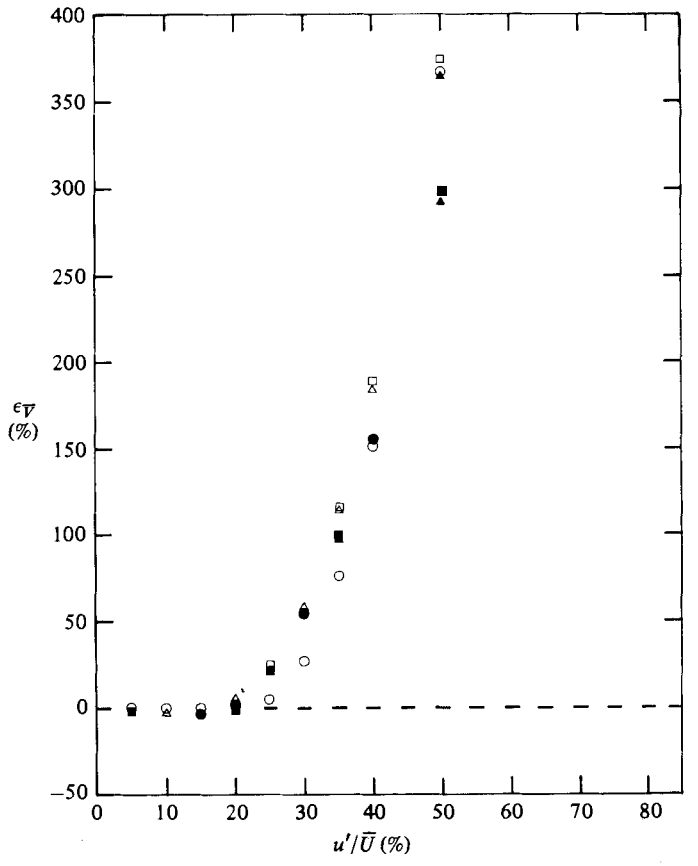


FIGURE 8. Effects of error-producing factors on $\epsilon_{\overline{V}}$ pertaining to the nonlinear X-wire response equations. (The relevant parameters are the same as in figure 5, and the symbols have the same meaning.)

whereas the other applicable factors, viz $w$ fluctuations and axial cooling, have little or no effect on these error quantities (figures 5 and 6).

(6) When $u'/\overline{U}$ lies between about 15% and about 25%, the dominant error-producing factors are, in order of importance, $w$ fluctuations, wire separation and $A$-variations.

(7) When $u'/\overline{U}$ is greater than about 20%, the dominant error-producing factors are, in order of importance, $w$ fluctuations, rectification, wire separation and $A$-variations.

(8) Axial cooling is of significance only with respect to estimates of $v'$ and, to a lesser extent, estimates of $\overline{uv}$, when $k = 0.1$ (figures 10 and 11 compared with figures 5–9).†

(9) $A$-variations will have a marked influence on the $v$-SDP (figure 6) but a relatively insignificant influence on the $u$-SDP (figure 5).

(10) When rectification alone is considered, the $u$-SDP and the $v$-SDP are essentially equal for all relevant values of $u'/\overline{U}$ (figures 5 and 6). This stems from

† Other error data obtained by us (which are not presented here) demonstrate that this observation applies also when $k = 0.15$. Furthermore, it is consistent with the error data of Tutu & Chevray (1975) pertaining to $k = 0.15$ and the findings of Champagne & Sleicher (1967).

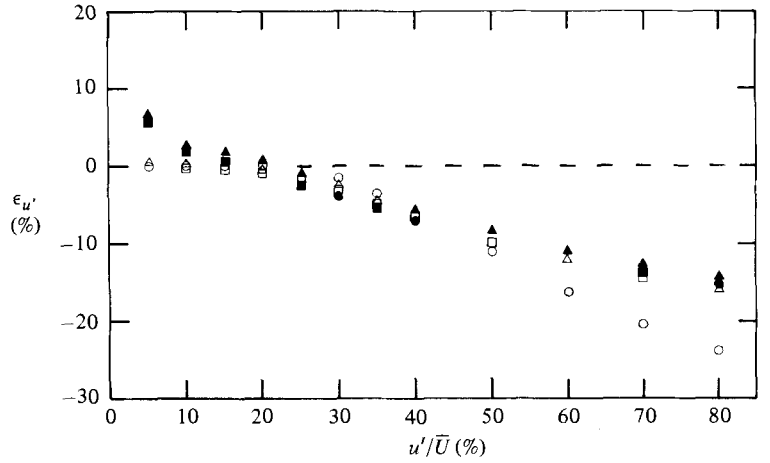


FIGURE 9. Effects of error-producing factors on $\epsilon_{u'}$ pertaining to the nonlinear X-wire response equations. (The relevant parameters are the same as in figure 5, and the symbols have the same meaning.)

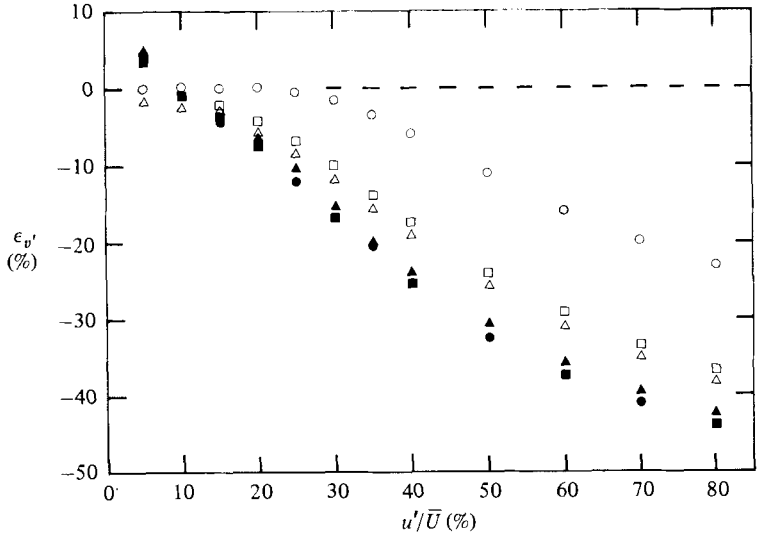


FIGURE 10. Effects of error-producing factors on $\epsilon_{v'}$ pertaining to the nonlinear X-wire response equations. (The relevant parameters are the same as in figure 5, and the symbols have the same meaning.)

the fact that the following relationship must hold for any 45° X-wire probe when only rectification is present:

$$\overline{(u_e - u_t)^2} = \overline{(v_e - v_t)^2}.$$

On the basis of this relationship and the definition of the SDP (see §5), the ratio of the $u$-SDP to the $v$-SDP should be equal to the ratio of $\overline{v_t^2}$, to $\overline{u_t^2}$,† so that, if $v_t'/u_t' = 1.0$ as in the present situation, then the $u$-SDP should be identical with the $v$-SDP.

(11) The effect of $w$-fluctuations on the $u$-SDP is more pronounced than it is on the $v$-SDP, the more so, the greater the value of $u'/\bar{U}$. In consequence, as $u'/\bar{U}$

† Results pertaining to $v_t'/u_t' = 0.8$, obtained by us, are entirely consistent with this.

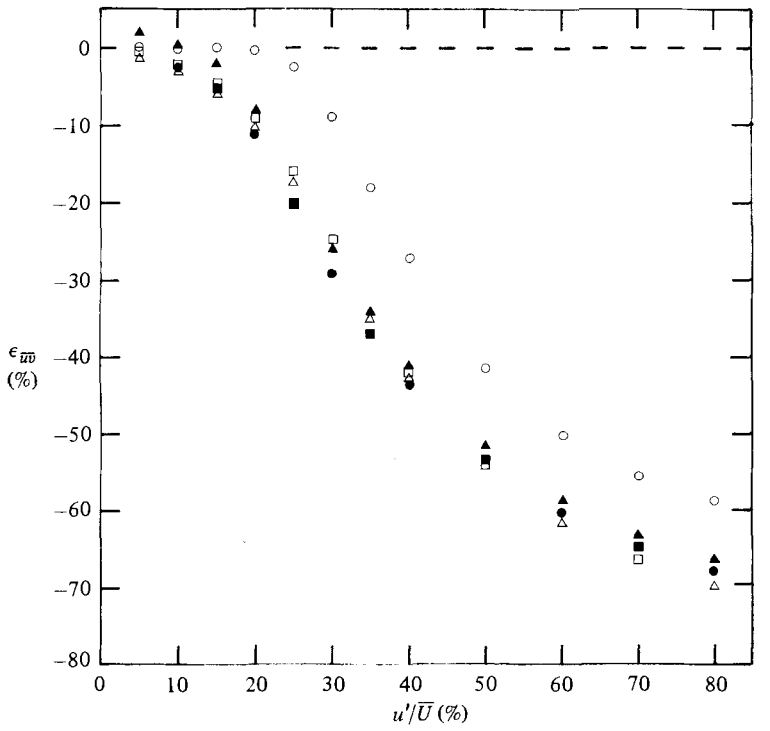


FIGURE 11. Effects of error-producing factors on $\epsilon_{\overline{uv}}$ pertaining to the nonlinear X-wire response equations. (The relevant parameters are the same as in figure 5, and the symbols have the same meaning.)

increases, the $u$-SDP increases at a faster rate than does the $v$-SDP (figures 5 and 6).

(12) When $u'/\overline{U}$ is greater than about 10 %, wire separation and $w$-fluctuations each cause the $u$-SDP to increase, but they each cause $|\epsilon_{u'}|$ to decrease. For instance, when $u'/\overline{U} = 80\,\%$, $w$-fluctuations can lead to an increase of about 30 % in the $u$-SDP, and wire separation to a further increase of about 3 % ; in contrast, $w$-fluctuation can effect a decrease of about 8 % in $|\epsilon_{u'}|$, and wire separation a further decrease of about 3 %. This clearly underscores the observation, made in §5, that the error in the r.m.s. value of an estimated velocity signal is not the proper measure of the distortion associated with that signal.

### 6.3. *Comparison of basic* X*-wire and* 3*-wire error data*

The information contained in §6.2, in conjunction with that given by Kawall *et al.* (1983), demonstrates that the main factors capable of adversely affecting X-wire results are calibration errors, wire separation and $w$-fluctuations when $u'/\overline{U}$ is less than about 20 %, and wire separation, $w$-fluctuations and rectification when $u'/\overline{U}$ is in excess of this value. We can effectively eliminate the distortion in estimated $U$- and $V$-signals resulting from calibration errors and wire separation by using the optimum $n$-value and by making $S_w$ sufficiently small relative to $\lambda_g$. But, for the X-wire configuration, signal distortion caused by $w$-fluctuations and/or rectification is unavoidable. In contrast, with the present 3-wire technique, signal distortion due to $w$-fluctuations can be completely eliminated, as is evident from equations (2.14) and (2.15), and that due to rectification will not occur until, as figure 4 indicates, $u'/\overline{U}$ is about 35 %. The implication of this is clear. For any turbulence-intensity level

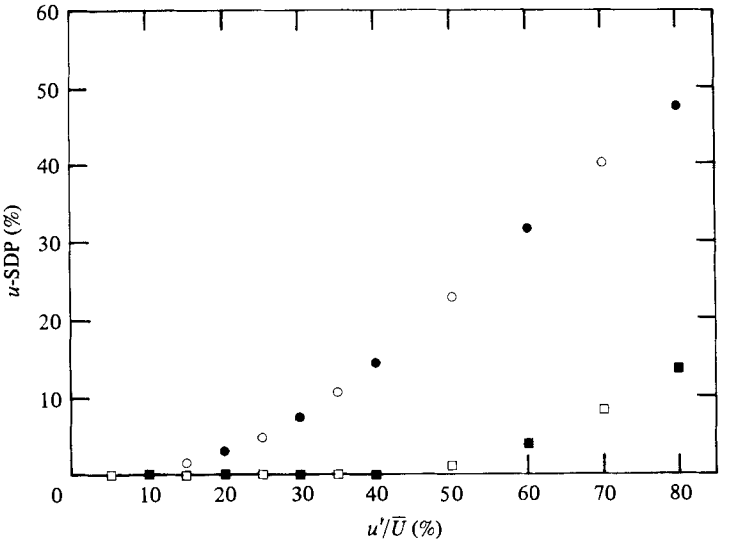


FIGURE 12. Comparison of $u$-SDP values pertaining to the nonlinear X-wire and 3-wire response equations. Relevant parameters: $\overline{V} = \overline{W} = \overline{uw} = \overline{vw} = 0$, $v'/u' = w'/u' = 0.8$, $\rho_{uv} = 0.3$, $k = 0.1$. Rectification and $w$-fluctuations present: ○, present X-wire results; □, present 3-wire results; – – –, X-wire results of Tutu & Chevray (1975). Preceding factors plus axial cooling present: ●, present X-wire results; ■, present 3-wire results.

between about 10% and a value in excess of 35%, the magnitudes of all error quantities will be smaller when this 3-wire technique is used than they will be when any X-wire technique is used. A basic indication of the extent of the reduction in these magnitudes that can be effected through the use of the former technique is provided by figures 12–17. In these figures, we have plotted the following: $u$-SDP, $v$-SDP, $\epsilon_U$, $\epsilon_{u'}$, $\epsilon_{v'}$ and $\epsilon_{\overline{uv}}$ data obtained by means of the 3-wire response equations (2.4)–(2.6), subject to (*a*) the presence of $w$-fluctuations and rectification, and subject to (*b*) the presence of $w$-fluctuations, rectification and axial cooling (with $k = 0.1$); corresponding data obtained by means of the X-wire response equations (2.4) and (2.5); relevant $\epsilon_U$, $\epsilon_{u'}$, $\epsilon_{v'}$ and $\epsilon_{\overline{uv}}$ data that have been reported by Tutu & Chevray (1975). All these data were determined with $W = uv = uw = V/U = 0$, $v'/u' = w'/u' = 0.8$ and $\rho_{uv} = 0.3$.

The figures confirm that results determined with the 3-wire technique are likely to be more reliable than those determined with any X-wire technique, once $u'/\overline{U}$ is greater than about 15%. Moreover, as anticipated, the present $\epsilon_{\overline{U}}$, $\epsilon_{u'}$, $\epsilon_{v'}$ and $\epsilon_{\overline{uv}}$ data obtained by means of the aforementioned X-wire equations subject to (*a*) are in excellent agreement with the corresponding data found by Tutu & Chevray (1975).

### 6.4. *Assessment of various HWA techniques*

With a view to assessing not only the present 3-wire HWA technique but also current HWA techniques that rely on the use of mean and linearized response equations, nonlinear normal response equations and nonlinear X-wire response equations, we carried out a computer error analysis based on: (*A*) the mean and linearized normal-wire response equations, (2.40) and (2.41); (*B*) the nonlinear normal-wire response equation, (2.6); (*C*) the mean and linearized X-wire response equations (2.34)–(2.37); (*D*) the nonlinear X-wire response equations (2.4) and (2.5); and (*E*) the nonlinear 3-wire response equations (2.4)–(2.6).

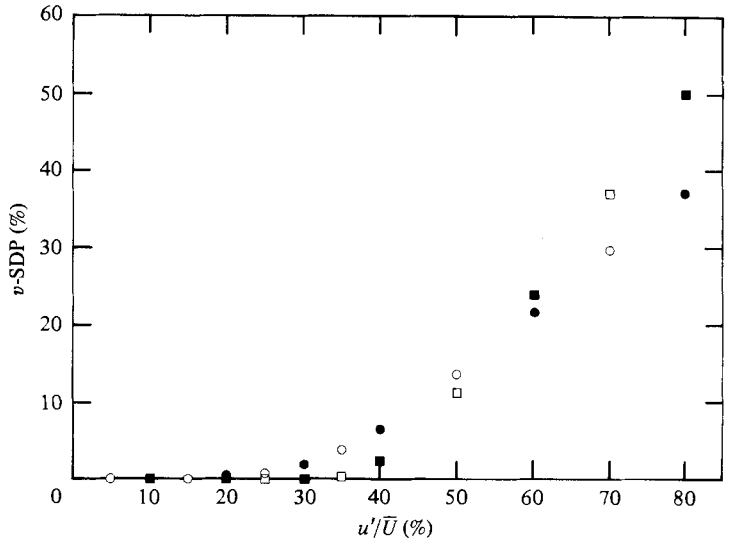


FIGURE 13. Comparison of $v$-SDP values pertaining to the nonlinear X-wire and 3-wire response equations. (The relevant parameters are the same as in figure 12, and the symbols have the same meaning.)

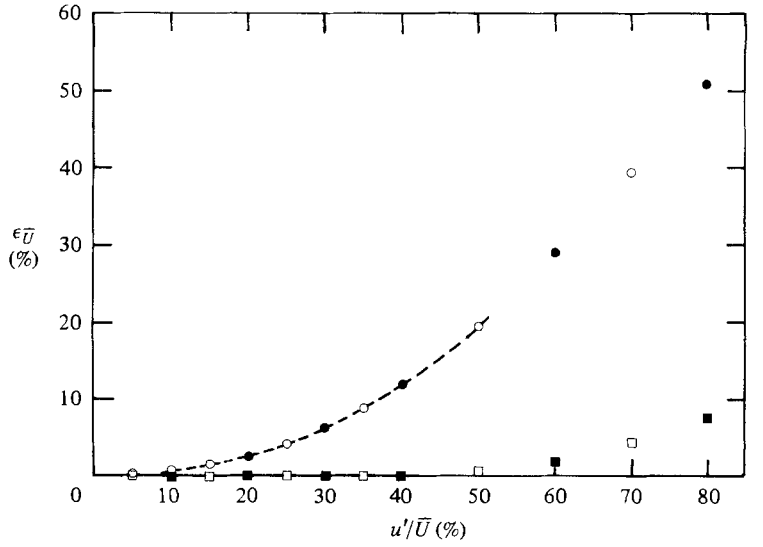


FIGURE 14. Comparison of $\epsilon_{\bar{U}}$ values pertaining to the nonlinear X-wire and 3-wire response equations. (The relevant parameters are the same as in figure 12, and the symbols have the same meaning.)

Furthermore, we calculated various error data with all six factors discussed in §6.2 present and using several sets of appropriate values of $\overline{U}$, $\overline{V}/\overline{U}$, $\rho_{uv}$ and $\Delta e_s'/e'$ (the wire separation parameter). Two values of $\Delta e_s'/e'$, corresponding to values of $S_w/\lambda_g$ of 0.1 and 0.2, were used. The values of $v'/u'$ and $w'/u'$ were each taken to be unity, the value of $k$ was taken to be 0.1 and the value of $\Delta e_c'/E_0$ (the calibration-error parameter) was taken to be 0.001, which, as implied in §4, is likely to be the maximum possible value of this parameter once optimum $n$-values are employed in the processing of HWA voltage signals.

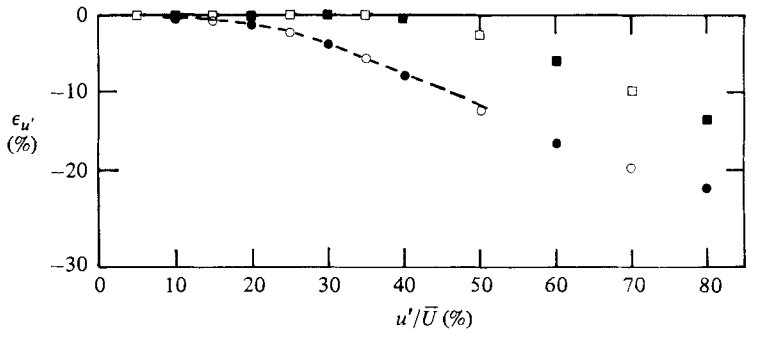


FIGURE 15. Comparison of $\epsilon_{u'}$ values pertaining to the nonlinear X-wire and 3-wire response equations. (The relevant parameters are the same as in figure 12, and the symbols have the same meaning.)

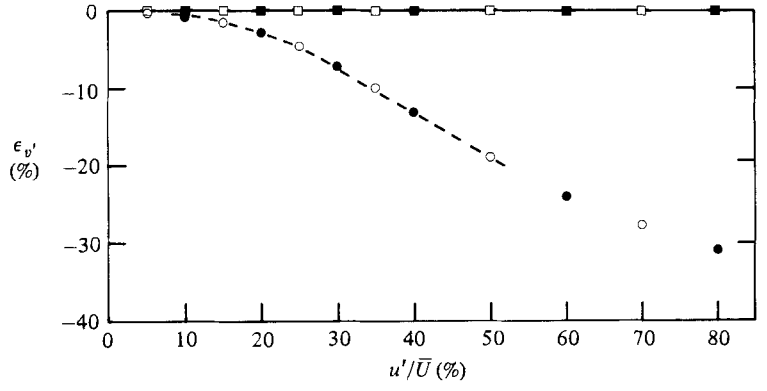


FIGURE 16. Comparison of $\epsilon_{v'}$ values pertaining to the nonlinear X-wire and 3-wire response equations. (The relevant parameters are the same as in figure 12, and the symbols have the same meaning.)

The essential results of the error analysis are presented in tables 1 and 2, an inspection of which reveals the following points.

(1) With respect to the present 3-wire technique, for any value of $u'/\overline{U}$ between about 10 % and about 35 %, the magnitudes of the $u$-SDP, the $v$-SDP, $\epsilon_{\overline{U}}$, $\epsilon_{\overline{V}}$, $\epsilon_{u'}$, $\epsilon_{v'}$, $\epsilon_{w'}$ and $\epsilon_{\overline{uv}}$ will be less than about 10 %; for any value of $u'/\overline{U}$ between about 35 % and about 45 %, the magnitudes of all these error quantities except perhaps $\epsilon_{\overline{V}}$ will be less than about 15 % ($|\epsilon_{\overline{V}}|$ may be in excess of this value); and for any value of $u'/\overline{U}$ between about 45 % and about 70 %, the magnitudes of the $u$-SDP, $\epsilon_{\overline{U}}$, $\epsilon_{u'}$, $\epsilon_{v'}$ and $\epsilon_{w'}$ will be less than 15 %.

(2) With respect to any X-wire technique, for values of $u'/\overline{U}$ greater than about 30 %, the magnitudes of all the error quantities in question except the $v$-SDP and $\epsilon_{u'}$ will be in excess of about 15 %; and for any value of $u'/\overline{U}$ greater than about 40 %, the magnitudes of all these quantities except $\epsilon_{u'}$ will be in excess of 20 %.

(3) When $u'/\overline{U}$ is less than about 25 %, the nonlinear X-wire response equations will yield much the same $U$-signals as will the corresponding mean and linearized response equations; and, when $u'/\overline{U}$ lies between about 5 % and about 25 %, the former equations will yield significantly more accurate $V$-signals than will the latter.

(4) With respect to any normal-wire technique, for values of $u'/\overline{U}$ up to about 45 %, the $u$-SDP, $|\epsilon_{\overline{U}}|$ and $|\epsilon_{u'}|$ will be less than about 15 %.

(5) When $u'/\overline{U}$ is greater than about 20 %, the nonlinear normal-wire response

| $\frac{u'}{\overline{U}}$ (%) | HWA response equation(s) | $\frac{S_w}{\lambda_g}$ | $u$-SDP (%) | $v$-SDP (%) | $\epsilon_{\overline{U}}$ (%) | $\epsilon_{\overline{V}}$ (%) | $\epsilon_{\overline{uv}}$ (%) | $\epsilon_{u'}$ (%) | $\epsilon_{v'}$ (%) | $\epsilon_{w'}$ (%) | $\epsilon_{u'/\overline{U}}$ (%) |
|---|---|---|---|---|---|---|---|---|---|---|---|
| 5 | (*A*) Mean & lin. norm. wire | — | 1.3 | — | 0.0 | — | — | 0.8 | — | — | 0.8 |
| | (*B*) nonlin. norm. wire | — | 2.4 | — | 0.1 | — | — | 1.1 | — | — | 0.9 |
| | (*C*) Mean & lin. X-wire | 0.2 | 2.8 | 6.6 | 0.1 | −5.6 | 1.5 | 1.7 | 1.8 | — | 1.6 |
| | (*D*) Nonlin. X-wire | 0.2 | 3.6 | 3.4 | 0.3 | −0.1 | 2.1 | 1.6 | 1.5 | — | 1.4 |
| | (*E*) Nonlin. 3-wire | 0.2 | 12.5 | 3.5 | 0.0 | 0.5 | −2.9 | 6.0 | 1.9 | 2.1 | 6.0 |
| | (*D*) Nonlin. X-wire | 0.1 | 2.2 | 1.8 | 0.3 | −0.1 | 0.4 | 0.9 | 0.7 | — | 0.6 |
| | (*E*) Nonlin. 3-wire | 0.1 | 11.0 | 1.9 | 0.0 | 0.3 | −1.2 | 5.3 | 1.1 | 0.4 | 5.3 |
| 10 | (*A*) Mean & lin. norm. wire | — | 1.0 | — | 0.1 | — | — | 0.4 | — | — | 0.3 |
| | (*B*) Nonlin. norm. wire | — | 1.0 | — | 0.5 | — | — | 0.0 | — | — | −0.5 |
| | (*C*) Mean & lin. X-wire | 0.2 | 3.7 | 6.0 | 0.3 | −23.4 | 4.3 | 2.1 | 1.2 | — | 1.8 |
| | (*D*) Nonlin. X-wire | 0.2 | 4.0 | 2.4 | 1.0 | −0.5 | 1.1 | 1.1 | 0.3 | — | 0.1 |
| | (*E*) Nonlin. 3-wire | 0.2 | 4.7 | 2.8 | 0.0 | 1.6 | −2.6 | 2.2 | 1.7 | 2.0 | 2.2 |
| | (*D*) Nonlin. X-wire | 0.1 | 2.5 | 0.9 | 1.0 | −0.6 | −0.7 | 0.3 | −0.5 | — | −0.7 |
| | (*E*) Nonlin. 3-wire | 0.1 | 3.1 | 1.0 | 0.0 | 0.5 | −0.9 | 1.5 | 0.6 | 0.4 | 1.5 |
| 20 | (*A*) Mean & lin. norm. wire | — | 3.1 | — | 0.6 | — | — | 0.7 | — | — | 0.1 |
| | (*B*) Nonlin. norm. wire | — | 1.9 | — | 2.0 | — | — | −1.1 | — | — | −3.1 |
| | (*C*) Mean & lin. X-wire | 0.2 | 9.9 | 7.5 | 1.6 | −86.8 | 0.1 | 2.5 | −3.0 | — | 0.9 |
| | (*D*) Nonlin. X-wire | 0.2 | 9.4 | 3.2 | 4.3 | 3.3 | −6.8 | −0.1 | −4.8 | — | −4.2 |
| | (*E*) Nonlin. 3-wire | 0.2 | 2.8 | 3.4 | −0.3 | 3.8 | −3.5 | 1.7 | 1.8 | 4.5 | 1.9 |
| | (*D*) Nonlin. X-wire | 0.1 | 7.8 | 1.6 | 4.3 | 2.5 | −8.8 | −1.0 | −5.7 | — | −5.0 |
| | (*E*) Nonlin. 3-wire | 0.1 | 1.3 | 1.0 | −0.2 | −1.4 | −1.9 | 1.1 | 0.2 | 3.5 | 1.2 |

| | | | | | | | | | | | |
|---|---|---|---|---|---|---|---|---|---|---|---|
| 30 | (*A*) Mean & lin. norm. wire | — | 7.1 | — | 1.4 | — | — | 1.4 | — | — | 0.1 |
| | (*B*) Nonlin. norm. wire | — | 4.3 | — | 4.7 | — | — | −2.7 | — | — | −7.0 |
| | (*C*) Mean & lin. X-wire | 0.2 | 21.0 | 12.0 | 5.5 | −101.5 | −24.6 | −0.2 | −13.6 | — | −5.4 |
| | (*D*) Nonlin. X-wire | 0.2 | 19.2 | 7.5 | 10.6 | 48.0 | −25.1 | −3.1 | −13.9 | — | −12.4 |
| | (*E*) Nonlin. 3-wire | 0.2 | 2.9 | 4.1 | −0.9 | 2.9 | −2.1 | 2.9 | 2.1 | 7.2 | 3.8 |
| | (*D*) Nonlin. X-wire | 0.1 | 17.7 | 6.0 | 10.5 | 46.6 | −26.9 | −4.0 | −14.8 | — | −13.1 |
| | (*E*) Nonlin. 3-wire | 0.1 | 1.5 | 1.1 | −0.8 | −6.4 | −1.0 | 2.3 | 0.1 | 6.7 | 3.2 |
| 40 | (*A*) Mean & lin. norm. wire | — | 13.2 | — | 2.8 | — | — | 1.4 | — | — | −1.4 |
| | (*B*) Nonlin. norm. wire | — | 7.9 | — | 8.5 | — | — | −5.2 | — | — | −12.6 |
| | (*C*) Mean & lin. X-wire | 0.2 | 33.5 | 19.3 | 12.1 | −47.8 | −45.2 | −3.3 | −24.2 | — | −13.7 |
| | (*D*) Nonlin. X-wire | 0.2 | 30.3 | 14.3 | 19.6 | 126.7 | −40.3 | −6.1 | −22.5 | — | −21.5 |
| | (*E*) Nonlin. 3-wire | 0.2 | 3.2 | 7.1 | −1.5 | 29.1 | −10.1 | 1.9 | 2.6 | 7.3 | 3.5 |
| | (*D*) Nonlin. X-wire | 0.1 | 29.0 | 12.9 | 19.5 | 125.0 | −41.7 | −7.0 | −23.5 | — | −22.1 |
| | (*E*) Nonlin. 3-wire | 0.1 | 1.7 | 3.6 | −1.4 | 15.6 | −9.2 | 1.5 | 0.4 | 7.2 | 3.0 |
| 50 | (*A*) Mean & lin. norm. wire | — | 19.2 | — | 5.7 | — | — | −2.2 | — | — | −7.5 |
| | (*B*) Nonlin. norm. wire | — | 13.0 | — | 13.7 | — | — | −8.6 | — | — | −19.7 |
| | (*C*) Mean & lin. X-wire | 0.2 | 45.7 | 28.1 | 21.0 | 64.1 | −57.6 | −6.5 | −32.3 | — | −22.8 |
| | (*D*) Nonlin. X-wire | 0.2 | 41.4 | 22.2 | 30.6 | 231.5 | −51.0 | −8.9 | −29.4 | — | −30.3 |
| | (*E*) Nonlin. 3-wire | 0.2 | 4.5 | 17.3 | −1.3 | 148.2 | −26.1 | −1.4 | 3.4 | 6.3 | −0.1 |
| | (*D*) Nonlin. X-wire | 0.1 | 40.2 | 20.9 | 30.5 | 229.7 | −52.2 | −9.7 | −30.4 | — | −30.8 |
| | (*E*) Nonlin. 3-wire | 0.1 | 2.9 | 12.3 | −1.3 | 132.5 | −25.5 | −1.6 | 0.6 | 6.6 | −0.3 |
| 60 | (*A*) Mean & lin. norm. wire | — | 26.0 | — | 10.3 | — | — | −7.0 | — | — | −15.7 |
| | (*B*) Nonlin. norm. wire | — | 19.3 | — | 20.2 | — | — | −12.4 | — | — | −27.1 |
| | (*C*) Mean & lin. X-wire | 0.2 | 56.6 | 36.6 | 31.7 | 220.4 | −64.7 | −9.5 | −38.1 | — | −31.2 |
| | (*D*) Nonlin. X-wire | 0.2 | 51.7 | 29.9 | 43.2 | 353.9 | −58.2 | −11.3 | −34.6 | — | −38.1 |
| | (*E*) Nonlin. 3-wire | 0.2 | 7.4 | 30.5 | 0.1 | 355.6 | −40.8 | −5.8 | 3.2 | 5.2 | −5.9 |
| | (*D*) Nonlin. X-wire | 0.1 | 50.6 | 28.8 | 43.0 | 352.1 | −59.2 | −12.1 | −35.6 | — | −38.5 |
| | (*E*) Nonlin. 3-wire | 0.1 | 5.7 | 25.7 | −0.1 | 331.5 | −39.7 | −5.8 | 0.7 | 5.7 | −5.7 |
| 70 | (*A*) Mean & lin. norm. wire | — | 33.5 | — | 16.2 | — | — | −11.6 | — | — | −23.9 |
| | (*B*) Nonlin. norm. wire | — | 26.1 | — | 27.9 | — | — | −15.9 | — | — | −34.2 |
| | (*C*) Mean & lin. X-wire | 0.2 | 66.3 | 44.3 | 43.5 | 407.5 | −68.8 | −11.9 | −42.2 | — | −38.6 |
| | (*D*) Nonlin. X-wire | 0.2 | 61.1 | 37.2 | 56.9 | 484.2 | −63.0 | −13.3 | −38.4 | — | −44.7 |
| | (*E*) Nonlin. 3-wire | 0.2 | 11.7 | 44.1 | 2.6 | 607.0 | −50.7 | −10.3 | 3.2 | 4.2 | −12.6 |
| | (*D*) Nonlin. X-wire | 0.1 | 60.0 | 36.1 | 56.7 | 482.4 | −63.8 | −14.0 | −39.5 | — | −45.1 |
| | (*E*) Nonlin. 3-wire | 0.1 | 9.9 | 38.9 | 2.2 | 587.5 | −50.3 | −10.2 | 0.6 | 4.9 | −12.2 |

TABLE 1. Errors associated with HWA measurements; $\overline{U} = 10$ m s$^{-1}$, $\overline{V}/\overline{U} = 0.01$, $v'/u' = w'/u' = 1.0$, $\rho_{uv} = 0.3$

| $\frac{u'}{\overline{U}}$ (%) | HWA response equation(s) | $\frac{S_w}{\lambda_g}$ | $u$-SDP (%) | $v$-SDP (%) | $\epsilon_{\overline{U}}$ (%) | $\epsilon_{\overline{V}}$ (%) | $\epsilon_{\overline{uv}}$ (%) | $\epsilon_{u'}$ (%) | $\epsilon_{v'}$ (%) | $\epsilon_{w'}$ (%) | $\epsilon_{u'/\overline{U}}$ (%) |
|---|---|---|---|---|---|---|---|---|---|---|---|
| 5 | (*A*) Mean & lin. norm. wire | — | 4.1 | — | 0.0 | — | — | 2.2 | — | — | 2.2 |
| | (*B*) Nonlin. norm. wire | — | 3.6 | — | 0.1 | — | — | 1.7 | — | — | 1.5 |
| | (*C*) Mean & lin. X-wire | 0.2 | 4.9 | 7.3 | 0.1 | −5.4 | 1.8 | 3.1 | 2.1 | — | 3.0 |
| | (*D*) Nonlin. X-wire | 0.2 | 4.4 | 4.2 | 0.3 | 0.0 | 2.1 | 2.0 | 1.9 | — | 1.8 |
| | (*E*) Nonlin. 3-wire | 0.2 | 18.4 | 4.4 | 0.0 | 0.6 | −3.1 | 8.8 | 2.4 | 1.9 | 8.8 |
| | (*D*) Nonlin. X-wire | 0.1 | 2.9 | 2.6 | 0.3 | 0.0 | 0.5 | 1.2 | 1.1 | — | 1.0 |
| | (*E*) Nonlin. 3-wire | 0.1 | 16.9 | 2.7 | 0.0 | 0.4 | −1.5 | 8.1 | 1.5 | 0.2 | 8.1 |
| 10 | (*A*) Mean & lin. norm. wire | — | 1.1 | — | 0.1 | — | — | 0.4 | — | — | 0.3 |
| | (*B*) Nonlin. norm. wire | — | 1.3 | — | 0.5 | — | — | 0.2 | — | — | −0.3 |
| | (*C*) Mean & lin. X-wire | 0.2 | 4.1 | 6.1 | 0.3 | −22.7 | 4.2 | 2.4 | 1.2 | — | 2.0 |
| | (*D*) Nonlin. X-wire | 0.2 | 4.2 | 2.7 | 1.0 | −0.6 | 1.3 | 1.3 | 0.4 | — | 0.2 |
| | (*E*) Nonlin. 3-wire | 0.2 | 6.2 | 3.0 | 0.0 | 1.6 | −2.8 | 2.9 | 1.8 | 1.8 | 2.9 |
| | (*D*) Nonlin. X-wire | 0.1 | 2.7 | 1.1 | 1.0 | −0.7 | −0.5 | 0.4 | −0.4 | — | −0.5 |
| | (*E*) Nonlin. 3-wire | 0.1 | 4.6 | 1.2 | 0.0 | 0.5 | −1.1 | 2.2 | 0.8 | 0.3 | 2.2 |
| 20 | (*A*) Mean & lin. norm. wire | — | 1.8 | — | 0.6 | — | — | 0.6 | — | — | 0.0 |
| | (*B*) Nonlin. norm. wire | — | 2.0 | — | 2.0 | — | — | −1.0 | — | — | −3.0 |
| | (*C*) Mean & lin. X-wire | 0.2 | 9.0 | 7.8 | 1.9 | −83.8 | −3.7 | 1.5 | −5.5 | — | −0.5 |
| | (*D*) Nonlin. X-wire | 0.2 | 10.0 | 3.9 | 4.5 | 0.6 | −7.8 | −0.5 | −6.4 | — | −4.7 |
| | (*E*) Nonlin. 3-wire | 0.2 | 3.6 | 3.5 | −0.4 | 0.6 | −4.0 | 2.7 | 1.3 | 7.4 | 3.2 |
| | (*D*) Nonlin. X-wire | 0.1 | 8.5 | 2.4 | 4.4 | −0.1 | −9.7 | −1.3 | −7.2 | — | −5.5 |
| | (*E*) Nonlin. 3-wire | 0.1 | 2.1 | 1.2 | −0.3 | −4.3 | −2.4 | 2.1 | −0.1 | 6.4 | 2.5 |
| 30 | (*A*) Mean & lin. norm. wire | — | 7.0 | — | 1.5 | — | — | 1.2 | — | — | −0.2 |
| | (*B*) Nonlin. norm. wire | — | 4.3 | — | 4.7 | — | — | −2.7 | — | — | −7.0 |
| | (*C*) Mean & lin. X-wire | 0.2 | 23.2 | 15.8 | 6.9 | −85.8 | −30.3 | −1.8 | −19.5 | — | −8.2 |
| | (*D*) Nonlin. X-wire | 0.2 | 21.9 | 11.6 | 11.5 | 46.5 | −28.1 | −3.8 | −18.2 | — | −13.8 |
| | (*E*) Nonlin. 3-wire | 0.2 | 5.7 | 9.5 | −1.9 | 4.7 | −5.6 | 6.5 | 2.3 | 13.5 | 8.6 |
| | (*D*) Nonlin. X-wire | 0.1 | 20.6 | 10.2 | 11.5 | 45.3 | −29.5 | −4.6 | −19.1 | — | −14.4 |
| | (*E*) Nonlin. 3-wire | 0.1 | 4.4 | 6.7 | −1.8 | −4.6 | −4.1 | 6.1 | 0.6 | 13.1 | 8.1 |

| | | | | | | | | | | | |
|---|---|---|---|---|---|---|---|---|---|---|---|
| 40 | (*A*) Mean & lin. norm. wire | — | 12.7 | — | 3.1 | — | — | 1.0 | — | — | −2.0 |
| | (*B*) Nonlin. norm. wire | — | 7.9 | — | 8.5 | — | — | −5.2 | — | — | −12.6 |
| | (*C*) Mean & lin. X-wire | 0.2 | 35.4 | 25.1 | 14.7 | −59.6 | −48.0 | −4.0 | −31.2 | — | −16.3 |
| | (*D*) Nonlin. X-wire | 0.2 | 33.1 | 20.2 | 21.3 | 101.4 | −42.1 | −6.2 | −28.1 | — | −22.7 |
| | (*E*) Nonlin. 3-wire | 0.2 | 7.1 | 14.7 | −3.4 | 11.6 | −13.7 | 5.6 | 3.6 | 14.3 | 9.3 |
| | (*D*) Nonlin. X-wire | 0.1 | 31.9 | 19.0 | 21.2 | 99.9 | −43.3 | −6.9 | −29.0 | — | −23.2 |
| | (*E*) Nonlin. 3-wire | 0.1 | 5.9 | 11.2 | −3.4 | −3.8 | −12.1 | 5.3 | 1.6 | 14.3 | 8.9 |
| 50 | (*A*) Mean & lin. norm. wire | — | 18.7 | — | 6.0 | — | — | −2.6 | — | — | −8.2 |
| | (*B*) Nonlin. norm. wire | — | 13.0 | — | 13.7 | — | — | −8.6 | — | — | −19.6 |
| | (*C*) Mean & lin. X-wire | 0.2 | 46.3 | 34.1 | 24.3 | 10.4 | −59.5 | −6.4 | −39.2 | — | −24.7 |
| | (*D*) Nonlin. X-wire | 0.2 | 43.3 | 28.4 | 32.9 | 175.5 | −52.3 | −8.4 | −35.2 | — | −31.1 |
| | (*E*) Nonlin. 3-wire | 0.2 | 8.6 | 24.4 | −3.8 | 111.5 | −31.0 | 1.3 | 4.2 | 12.9 | 5.4 |
| | (*D*) Nonlin. X-wire | 0.1 | 42.2 | 27.3 | 32.8 | 174.0 | −53.3 | −9.1 | −36.2 | — | −31.5 |
| | (*E*) Nonlin. 3-wire | 0.1 | 7.2 | 19.7 | −3.9 | 92.9 | −29.8 | 1.2 | 2.2 | 13.2 | 5.3 |
| 60 | (*A*) Mean & lin. norm. wire | — | 25.5 | — | 10.7 | — | — | −7.4 | — | — | −16.3 |
| | (*B*) Nonlin. norm. wire | — | 19.3 | — | 20.2 | — | — | −12.4 | — | — | −27.1 |
| | (*C*) Mean & lin. X-wire | 0.2 | 56.1 | 42.0 | 35.5 | 127.8 | −66.5 | −9.0 | −44.7 | — | −32.8 |
| | (*D*) Nonlin. X-wire | 0.2 | 52.6 | 35.7 | 45.8 | 272.3 | −59.3 | −10.5 | −40.3 | — | −38.6 |
| | (*E*) Nonlin. 3-wire | 0.2 | 11.1 | 36.5 | −2.9 | 307.5 | −46.4 | −4.0 | 4.3 | 11.2 | −1.2 |
| | (*D*) Nonlin. X-wire | 0.1 | 51.6 | 34.6 | 45.7 | 270.7 | −60.1 | −11.2 | −41.2 | — | −39.0 |
| | (*E*) Nonlin. 3-wire | 0.1 | 9.7 | 31.6 | −3.1 | 285.0 | −45.4 | −4.0 | 2.1 | 11.6 | −0.9 |
| 70 | (*A*) Mean & lin. norm. wire | — | 32.9 | — | 16.6 | — | — | −11.9 | — | — | −24.5 |
| | (*B*) Nonlin. norm. wire | — | 26.1 | — | 27.9 | — | — | −15.9 | — | — | −34.2 |
| | (*C*) Mean & lin. X-wire | 0.2 | 65.2 | 48.7 | 47.7 | 274.1 | −70.1 | −11.2 | −48.5 | — | −39.9 |
| | (*D*) Nonlin. X-wire | 0.2 | 61.2 | 42.1 | 59.7 | 381.1 | −63.6 | −12.4 | −43.9 | — | −45.2 |
| | (*E*) Nonlin. 3-wire | 0.2 | 15.0 | 48.3 | −0.7 | 556.0 | −56.7 | −9.2 | 4.1 | 9.6 | −8.5 |
| | (*D*) Nonlin. X-wire | 0.1 | 60.2 | 41.2 | 59.6 | 379.4 | −64.4 | −13.1 | −44.9 | — | −45.5 |
| | (*E*) Nonlin. 3-wire | 0.1 | 13.4 | 43.1 | −1.1 | 541.5 | −56.5 | −9.0 | 1.9 | 10.2 | −8.0 |

TABLE 2. Errors associated with HWA measurements: $\overline{U} = 2$ m s$^{-1}$, $\overline{V}/\overline{U} = 0.01$, $v'/u' = w'/u' = 1.0$, $\rho_{uv} = 0.3$

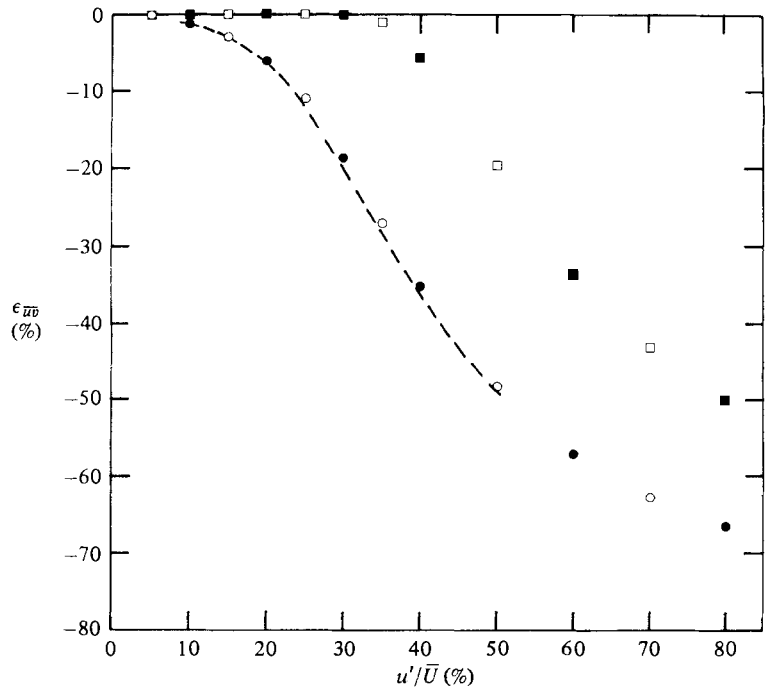


FIGURE 17. Comparison of $\epsilon_{\overline{uv}}$ values pertaining to the nonlinear X-wire and 3-wire response equations. (The relevant parameters are the same as in figure 12, and the symbols have the same meaning.)

equation will yield significantly more accurate $u$-signals than will the corresponding linearized response equation, but significantly less accurate $\overline{U}$-estimates than will the corresponding mean response equation.

(6) The $U$-signals obtained via the normal-wire response equations will be significantly more accurate than those obtained via the X-wire equations when $u'/\overline{U}$ is greater than about 10 %.

(7) The $U$-signals obtained via the 3-wire response equations will be significantly more accurate than those obtained via the normal-wire equations when $u'/\overline{U}$ is greater than about 30 % for flow situations in which $S_w/\lambda_g$ is about 0.1, and when $u'/\overline{U}$ is greater than about 40 % for flow situations in which $S_w/\lambda_g$ is about 0.2.

(8) When $u'/\overline{U}$ is less than about 45 %, the mean and linearized normal-wire response equations will yield the most accurate $u'/\overline{U}$ estimates, with the values of $\epsilon_{u'/\overline{U}}$ resulting from the use of these equations probably not exceeding about 5 %. And when $u'/\overline{U}$ is greater than about 45 %, the 3-wire response equations will yield the most accurate $u'/\overline{U}$ estimates, with the values of $\epsilon_{u'/\overline{U}}$ resulting from the use of these equations probably not exceeding about 10 % if $u'/\overline{U}$ is less than about 70 %.

(9) For any value of $u'/\overline{U}$ greater than about 35 %, $u'/\overline{U}$ values obtained via the X-wire response equations will be very much smaller than they should be – the more so the greater $u'/\overline{U}$ is beyond 35 %. For instance, if the actual $u'/\overline{U}$ value is 70 %, 'X-wire' $u/\overline{U}$ values are not likely to be much in excess of about 50 %.

(10) For any value of $u'/\overline{U}$ greater than about 25 %, values of the $v'/u'$ and $w'/u'$ ratios obtained via the X-wire equations will be at least 10 % smaller than they should

be, so that for instance, when $u'/\overline{U}$ is 30 %, if the 'X-wire' value of $v'/u'$ is 0.8, then its actual value is likely to be about 0.9. This implies that with respect to the continuously turbulent regions of jets, where $u'/\overline{U}$ values are usually about 25 %, the 'X-wire' values of the above ratios that have been obtained to date – such as those reported by Gutmark & Wygnanski (1976) for a plane jet and by Wygnanski & Fiedler (1969) for an axisymmetric jet – are at least 10 % too small; and hence these ratios are really not as far from unity as we have been led to believe on the strength of their 'X-wire' values.

(11) For any value of $u'/\overline{U}$, the nonlinear normal-wire response equation will yield much the same $u'$ value as the nonlinear X-wire response equations will, since – as tables 1 and 2 demonstrate – the *difference* between the relevant $\epsilon_{u'}$ values is not likely to exceed 5 %. This is entirely consistent with the comment made by Wygnanski & Fielder (1969), *vis-à-vis* their axisymmetric jet (in which $u'/\overline{U}$ values exceeded 25 %), that the $u'$ results which they obtained using an X-wire probe were identical with those which they obtained using a normal-wire probe.

On the basis of the abovementioned points, it can be concluded that (i) for $u'/\overline{U}$ values up to about 30 %, any normal-wire technique is likely to yield high-precision $U$-signals (i.e. signals whose mean values are accurate to within about 5 % and for which the SDPs are less than about 5 %), (ii) for any value of $u'/\overline{U}$ between about 30 % and about 70 %, the $U$-signals and all their statistical properties obtained by means of the present 3-wire technique will be reliable and significantly more accurate than those obtained by means of any normal wire technique, (iii) for $u'/\overline{U}$ values less than 10 %, any X-wire technique (or rotated single-wire technique) is likely to yield high-precision $U$- and $V$-signals, (iv) for $u'/\overline{U}$ values up to about 15 %, *nonlinear* X-wire techniques are capable of providing us with high-precision $U$- and $V$-signals, and (v) for any value of $u'/\overline{U}$ between about 15 % and about 40 %, the $U$- and $V$-signals (and all their statistical properties) obtained by means of the present 3-wire technique will be reliable and significantly more accurate than those obtained by means of *any* X-wire technique.

This research was supported by the Natural Sciences and Engineering Research Council of Canada through Grant No. A-2746.

## REFERENCES

BLACKWELDER, R. F. 1981 *Methods of Experimental Physics: Fluid Dynamics*, vol. 18, part A, p. 259. Academic.

BRADBURY, L. J. S. 1978 In *Proc. Dynamic Flow Conf., Marseille–Baltimore*, p. 489.

CHAMPAGNE, F. H. & SLEICHER, C. A. 1967 *J. Fluid Mech.* **28**, 177.

CHAMPAGNE, F. H., SLEICHER. C. A. & WEHRMANN, O. H. 1967 *J. Fluid Mech.* **28**, 153.

COLLIS, D. C. & WILLIAMS, M. J. 1959 *J. Fluid Mech.* **6**, 357.

DAVIES, A. E., KEFFER, J. F. & BAINES, W. D. 1975 *Phys. Fluids* **18**, 770.

FOSS, J. F. 1978 In *Proc. Dynamic Flow Conf., Marseille–Baltimore*, p. 983.

GUTMARK, E. & WYGNANSKI, I. 1976 *J. Fluid Mech.* **73**, 465.

HINZE, J. O. 1959 *Turbulence*. McGraw-Hill.

KAWALL, J. G., KEFFER, J. F. & SHOKR, M. 1983 *University of Toronto, Dept Mech. Engng Rep.* (to appear).

KEFFER, J. F., BUDNY, R. S. & KAWALL, J. G. 1978 *Rev. Sci. Instrum.* **49**, 1343.

LAKSHMINARAYANA, B. 1982 *TSI Q.* **8** (1), 3.
RODI, W. 1975 *DISA Info.* no. 17, p. 9.
TUTU, N. K. & CHEVRAY, R. 1975 *J. Fluid Mech.* **71**, 785.
WYGNANSKI, I. & FIEDLER, H. E. 1969 *J. Fluid Mech.* **38**, 577.
WYGNANSKI, I. & FIEDLER, H. E. 1970 *J. Fluid Mech.* **41**, 327.